

**EVALUATING THE THERMAL STRESS RESPONSE
OF SOUTH AFRICAN ABALONE, *HALIOTIS MIDAE*,
TO BIOGEOGRAPHICAL TEMPERATURE
VARIABILITY**

By

SHARON KHUZWAYO

Submitted in fulfilment of the academic requirements for the degree of
Master of Science in the School of Life Sciences,
University of KwaZulu-Natal, Durban

February 2014

As the candidate's supervisor I have approved this dissertation for submission.

Signed: _____



Name: André Vosloo

Date: 2014/02/03

ABSTRACT

A gradient of sea temperatures is created along the South African coastline by the confluence of the cold Benguela Current on the West coast with the warm Agulhas Current on the East coast. This temperature gradient allows for an assortment of species to occupy the variety of microenvironments occurring in this area. Amongst these species is commercially important South African abalone, *Haliotis midae*, which although being capable of existing across this wide range of temperatures grows larger on the cooler West coast. Abalone reared on the warmer East coast however, experience greater mortalities especially during the more thermally variable summer months. The aim of the study was thus to assess the zone of tolerance for *H. midae* by exposing abalone to fluctuating temperatures in an attempt to model environmental temperature instability, a scenario which may likely be worsened by global climate change.

Animals from the West and East coasts were exposed to two thermal treatments of fluctuating temperatures with the first group being kept at $16^{\circ}\text{C}\pm 2$ and the second group kept at $16^{\circ}\text{C}\pm 4$. The control group was maintained at a constant 16°C indicating that the mean temperature experienced by all three groups was 16°C . Oxygen consumption, nitrogen excretion and O:N ratio were assessed at the organismal level to give an indication of metabolic rate, amount of protein excreted and type of metabolic substrate utilized respectively. At the biochemical level, D-lactate accumulation was quantified to indicate whether metabolism was proceeding aerobically or anaerobically. Heat shock protein 70 (Hsp70) expression and degree of carbonylation were analyzed at the proteomic level with *Hsp70* also being assessed at the transcriptomic level. All biological responses were measured at days 1, 3, 7 and 14 of the two week exposure.

Oxygen consumption rates were significantly elevated on day 14 when comparing treatment group animals to control group animals of the same biogeographic region. $P < 0.05$ for both treatment groups from the West coast, while $P < 0.001$ for the East coast treatment groups. The ammonia excretion rates of the West coast animals were significantly lower than those of the controls at day 14 with $P < 0.001$ for both treatment groups, while ammonia excretion rates were elevated in East coast animals at day 14, although not significantly. Trends similar to those seen for ammonia excretion rates were exhibited by O:N ratios. West coast animals showed lower than control O:N ratios at day 14 ($P < 0.01$ for both treatment groups) while East coast animals displayed higher than control values ($P < 0.05$ only for the $16^{\circ}\text{C}\pm 2$ group) at day 14. D-lactate, having been detected only for the West coast animals, showed no significant differences

but large degrees of variation were noted on days 1 and 7. Carbonylation was evident for animals from both biogeographic regions with baseline carbonyl accumulation for East coast animals being greater (non-significantly) than that of the West coast animals. The *hsp70* gene expression remained low for both biogeographic groups with West coast animals appearing to show slight elevations in expression at days 1 and 7, days which also displayed high degrees of variability.

The West coast animals appeared to be better suited to coping with the thermal fluctuations, as they not only transiently reduced oxygen consumption rate to reduce ROS production, but also utilized the assistance of the D-lactate pathway possibly to maintain metabolism, both of which were not observed in the East coast animals. Although West coast abalone seemed to have slightly elevated *hsp70* expression (suggestive of a repair response) when compared to their East counterparts, both groups of abalone were shown to have incurred notable amounts of protein damage (i.e. carbonylation). This suggests impairments in both protective and repair responses for animals from both biogeographic regions. The lack or attenuation of physiological responses noted in East coast abalone may be due to limitations in thermal adaptation but subsequent studies are required to confirm this notion.

The information obtained from this study may assist in providing an insight into the mechanisms responsible for thermal limitation in *H. midae* and how this species is likely to respond to future periods of thermal instability which may be worsened by global climate change. An understanding of the processes leading up to limitations may potentially assist the abalone aquaculture industry in altering culturing practices early on to support optimal performance in abalone.

PREFACE

The experimental work described in this dissertation was carried out in the School of Life Sciences, University of KwaZulu-Natal, Durban, from January 2012 to December 2013, under the supervision of Doctor André Vosloo.

These studies represent original work by the author and have not otherwise been submitted in any form for any degree or diploma to any tertiary institution. Where use has been made of the work of others it is duly acknowledged in the text.

2014/02/03

Sharon Khuzwayo (Candidate)

Date

DECLARATION OF PLAGIARISM

I, Sharon Khuzwayo, declare that

1. The research reported in this thesis, except where otherwise indicated, is my original research.
2. This thesis has not been submitted for any degree or examination at any other university.
3. This thesis does not contain other persons' data, pictures, graphs or other information, unless specifically acknowledged as being sourced from other persons.
4. This thesis does not contain other persons' writing, unless specifically acknowledged as being sourced from other researchers. Where other written sources have been quoted, then:
 - a. Their words have been re-written but the general information attributed to them has been referenced
 - b. Where their exact words have been used, then their writing has been placed in italics and inside quotation marks, and referenced.
5. This thesis does not contain text, graphics or tables copied and pasted from the Internet, unless specifically acknowledged, and the source being detailed in the thesis and in the References sections.

Signed:

LIST OF TABLES

Table 2.1: The average water quality values (shown with standard error) measured during the acclimation period as well as for the control tanks for the duration of exposures. Minimum and maximum water quality values given in brackets.	16
Table 2.2: Primer sequence information (Vosloo <i>et al.</i> , 2013).	25
Table 3.1: <i>P</i> -values for all biological responses measured, where $n = 6$ for all responses excluding D-lactate ($n = 5$) and carbonyl ($n = 4$) accumulation.	28
Table 3.2: The mean and standard error values for the control groups of the biological responses assessed (excluding <i>hsp70</i> gene expression), with $n = 6$ excepting for D-lactate ($n = 5$) and carbonyl ($n = 4$) accumulation.	29

LIST OF FIGURES

- Figure 1.1:** A map of the South African coastline illustrating the convergence of the Benguela and Agulhas Currents, along with the estimated species distribution of *Haliotis midae* (adapted from Proudfoot (2007) and <http://www.seos-project.eu/modules/oceancurrents/oceancurrents-c04-p05.html>). 2
- Figure 1.2:** Annual temperature profiles of a West coast based abalone farm (HIK) versus that of an East coast based farm (WCA). (From Vosloo A., 2013; unpublished). 3
- Figure 1.3:** Mean daily temperatures experienced at a West coast (HIK) and an East coast (WCA) based farm, taken over a 5 year period (From Vosloo A., 2013; unpublished). 4
- Figure 1.4:** The thermal window of aquatic animals as set by scope of aerobic performance. The peak of the curve displays the optimum temperature for aerobic performance (grey band) with points further from this indicating pejus temperatures (T_p) (blue bands), followed by critical temperatures (T_c) (green bands), and lastly denaturation temperatures (red band). Adapted from Pörtner and Farrell (2008). 6
- Figure 1.5:** Oxidative stress – i) Optimal conditions in a biological system where antioxidants (AOX) are in balance with the amount of reactive oxygen species (ROS) produced. ii) Unbalanced system where excess ROS production results in oxidative stress. iii) Unbalanced system where antioxidant depletion leads to oxidative stress. Adapted from Scandalios (2005). 7
- Figure 1.6:** Sites of tissue sampling (indicated by boxes) where the enzyme activities for D-lactate dehydrogenase (D-LDH) and tauroxine dehydrogenase (TDH) can be measured. Adapted from Gäde (1988). 9
- Figure 1.7:** The model for the activation of *hsp70* genes and the production of Hsp proteins in response to thermal stress denatured proteins. Adapted from Tomanek and Somero (2002). 12
- Figure 1.8:** Pathways that can generate carbonylation-prone protein species: 1) irregular protein production due to errors in translation, 2) irregular protein conformations as a result of defective chaperones, 3) abnormalities in protein conformations due to denaturing stresses, and 4) the hypothetical formation of carbonyls on idle enzymes which are put at risk as a result of inactivity. Once formed carbonylated proteins form aggregates which appear to inhibit proteolysis. Taken from Nyström (2005). 13

Figure 2.1: Temperature fluctuations as experienced by abalone exposed to the two experimental temperature regimes. Animals belonging to experimental group 16°C±2 were exposed to a minimum temperature of 14°C and a maximum temperature of 18°C; while experimental group 16°C±4 was exposed to a minimum temperature of 12°C and a maximum of 20°C. Sampling occurred prior to the commencement of temperature spikes (indicated by crosses) while oxygen consumption readings and ammonia samples were taken at the highest temperature that animals were exposed to in each experimental group (indicated by arrows)... 17

Figure 3.1: The oxygen consumption (MO₂) of exposed West (a) and East coast animals (b) normalized against that of the control animals for each respective region. Error bars denote standard error and significant differences are denoted by asterisks (*) where * indicates $P < 0.05$, ** indicates $P < 0.01$ and *** indicates $P < 0.001$ when comparing treatment groups to the control. Significant differences across regions are indicated by hash symbols (#) where # shows $P < 0.05$, ## shows $P < 0.01$ and ### shows $P < 0.001$. The color of the symbols corresponds to the treatment group as indicated by the key (n = 6 for the control and n = 5 for the treatment groups)..... 30

Figure 3.2: The ammonia excretion (MNH₃-N) of the exposed West (a) and East coast (b) animals normalized against that of the control group for each region. Asterisks (*) and hash symbols (#) denote the degree of significant differences ($P < 0.05$, $P < 0.01$ or $P < 0.001$) when comparing treatment groups to the control. Asterisks represent within population significances while hash symbols show across population differences. The treatment is indicated by the color of symbols as show by the key. Error bars indicate standard error (n = 6 for the controls while n = 3 for the treatment groups)..... 32

Figure 3.3: Oxygen: nitrogen (O:N) ratio of West (a) and East (b) coast animals using control values for normalization of treatments. Significant differences ($P < 0.05$, $P < 0.01$ or $P < 0.001$) are denoted by asterisks (*) or hash symbols (#) where colored symbols (see key) indicated differences between treatments and the control and black symbols show differences between treatment groups themselves. Standard error denoted by error bars (n = 6 for the controls and n = 3 for the treatments). 33

Figure 3.4: The D-lactate produced by the West coast animals normalized against that of the control animals. Error bars symbolize standard error (n = 5 for both treatments and control). .. 35

Figure 3.5: Representation of a dot blot indicating high background signal, shown with accompanying Ponceau S stained blot indicating the presence of protein. Illustration shows dot blot of samples taken from West coast reared abalone. 35

Figure 3.6: Amounts of carbonylated protein detected for West coast (a) and East coast (b) animals, normalized against their respective control values. Error bars indicate standard error (n = 4 for the treatments and controls).	36
Figure 3.7: Validation of the presence of the 28 S and 18 S rRNA subunits of intact RNA. RNA shown above extracted from the first biological repeat of the West coast (a) and East coast (b) samples. (MWM indicates molecular weight marker).	37
Figure 3.8: The <i>hsp70</i> levels (expressed relative to <i>coxIII</i>) of West coast (a) and East coast (b) animals . The relative expression of the treatment groups (16°C±2 and 16°C±4) is normalized to the control levels over the two week exposure and error bars denote standard error (n = 3).....	38
Figure A.2.4.1: Validation of the action and specificity of the Hsp70 primary antibody.	58
Figure A.2.4.2: Validation of effective transfer and presence of protein on Western blots.....	58
Figure A.2.4.3: Dot blot of a selected protein samples with accompanying Ponceau S stained blot. Dot blot image conveys high levels of background signal.....	59
Figure A.2.4.4: Dot blot from which no signal was detected as a result of extended washing. Presence of protein confirmed by Ponceau S stained blot.	60
Figure B.3.1: Protocol used to perform all qPCR reactions outlined by Vosloo <i>et al.</i> (2013) and created using the Eco™ Software (v3.0.16.0).....	64
Figure B.3.2: Fluorescence curves representing (a) <i>coxIII</i> and (b) <i>hsp70</i> amplification.	65
Figure B.4.1: i) Curves representing melt for (a) <i>hsp70</i> and (b) <i>coxIII</i> . ii) Accompanying melt temperature data (control data shown only) and validation by agarose gel electrophoresis showing <i>coxIII</i> (150 bp) and <i>hsp70</i> (200 bp) bands.....	66
Figure B.4.2: Assessment of efficiency curves for <i>coxIII</i> (a) where $R^2 = 0.9966$ with a corresponding reaction efficiency of 117.4%, and for <i>hsp70</i> (b) where $R^2 = 0.9851$ and had a corresponding reaction efficiency of 66.4%.....	67

LIST OF CONTENTS

ABSTRACT.....	ii
PREFACE.....	iv
DECLARATION OF PLAGIARISM.....	v
LIST OF TABLES.....	vi
LIST OF FIGURES.....	vii
LIST OF CONTENTS.....	x
ABBREVIATIONS.....	xiii
ACKNOWLEDGEMENTS.....	xv
1. INTRODUCTION.....	1
1.1. Thermal Stress in Marine Organisms.....	3
1.2. The Effects of Temperature on Aerobic Performance.....	5
1.3. The Consequences of Elevated Metabolic Rates.....	7
1.4. Anaerobic Metabolism.....	8
1.5. The End-Products of Protein Metabolism and Toxicity.....	9
1.6. The Stabilization and Destabilization of the Protein Pool.....	10
1.7. Aims and Objectives.....	13
2. MATERIALS AND METHODS.....	15
2.1. Collection and Acclimation.....	15
2.2. Exposure and Sampling.....	16
2.3. Oxygen Consumption Rates.....	18
2.4. Ammonia Excretion Rates.....	18
2.5. Oxygen: Nitrogen Ratio.....	19
2.6. D-Lactate Accumulation.....	19

2.7.	Dot Blotting.....	20
2.7.1.	Protein Extraction.....	20
2.7.2.	Protein Quantification	20
2.7.3.	Protein Blotting and Detection	21
2.8.	Oxidized Protein Assay	21
2.8.1.	Sample Preparation and Total Protein Content Determination	21
2.8.2.	Carbonylated Protein Content Assay	22
2.8.3.	Carbonylated Protein Content Calculation.....	22
2.9.	Conventional Polymerase Chain Reaction (PCR).....	23
2.9.1.	RNA Extraction and Integrity Assessment	23
2.9.2.	Complementary DNA (cDNA) Synthesis	24
2.9.3.	Conventional PCR.....	24
2.9.4.	PCR Product Electrophoresis	25
2.10.	Quantitative Real-Time PCR (qPCR)	25
2.11.	Statistical Analyses	26
3.	RESULTS	28
3.1.	Organismal Level Responses	28
3.1.1.	Oxygen Consumption Rates.....	29
3.1.2.	Ammonia Excretion Rates	31
3.1.3.	Oxygen: Nitrogen Ratios.....	33
3.2.	Biochemical Level Responses.....	34
3.2.1.	D-lactate Accumulation.....	34
3.3.	Proteomic Level Responses	35
3.3.1.	Stress Protein (Hsp70) Response	35
3.3.2.	Oxidized Protein Responses	36
3.4.	Transcriptomic Level Responses	37

3.4.1. RNA Integrity Validation.....	37
3.4.2. Relative <i>Hsp70</i> Expression	38
4. DISCUSSION	39
4.1. Metabolic Modification in Response to Thermal Stress	39
4.1.1. Organismal Level Adjustments	39
4.1.2. Biochemical Level Adjustments	42
4.1.3. Proteomic Level Adjustments	43
4.1.4. Transcriptomic Level Adjustments	44
4.2. Overall Aerobic Performance of West Coast vs East Coast Animals	45
4.3. Conclusion and Future Considerations.....	47
5. REFERENCE LIST.....	50
6. APPENDIX	55
A. Recipes	55
A.1. Phenol-Hypochlorite Method.....	55
A.2. Dot Blotting Procedure.....	56
A.3. RNA Extraction and Integrity Assessment.....	60
A.4. PCR Product Electrophoresis	62
B. MIQE Guidelines	63
B.1. Experimental Design	63
B.2. RNA Extraction and cDNA Synthesis.....	63
B.3. qPCR Protocol	64
B.4. qPCR Validation.....	65
B.5. Data Analysis.....	68

ABBREVIATIONS

ANOVA	Analysis of variance
AOX	Antioxidant(s)
BCA	Bicinchoninic acid
cDNA	Complementary deoxyribonucleic acid
DEPC	Diethylpyrocarbonate
D-GPT	D-glutamate-pyruvate transaminase
D-LDH	D-lactate dehydrogenase
DNPH	2,4-Dinitrophenylhydrazine (Brady's reagent)
EDTA	Ethylenediaminetetraacetic acid
ETC	Electron transport chain
HRP	Horse-radish peroxidase
HSE	Heat shock element
HSF1	Heat shock factor 1
Hsp	Heat shock protein
HSR	Heat shock response
IgG	Immunoglobulin G
kDa	Kilo Dalton
MIQE	Minimum information for publication of quantitative real-time PCR experiments
MO ₂	Specific oxygen consumption
MWM	Molecular weight marker
NAD ⁺	Nicotinamide adenine dinucleotide

NADP ⁺	Nicotinamide adenine dinucleotide phosphate
NTC	No template control
O:N	Oxygen:nitrogen
PBS	Phosphate-buffered saline
PO ₂	Partial oxygen pressure
PCR	Polymerase chain reaction
qPCR	Quantitative real-time polymerase chain reaction
ROS	Reactive oxygen species
RT	Reverse transcription
TBE	Tris-Borate EDTA
TBS	Tris-Buffered Saline
TBS-T	Tris-Buffered Saline – Tween20
T _c	Critical temperature
TCA	Trichloroacetic acid
T _d	Denaturation temperature
T _m	Melting temperature
T _p	Pejus temperature
WCA	Wild Coast Abalone

ACKNOWLEDGEMENTS

Firstly, I would like to thank my supervisor Dr André Vosloo for his continued assistance and supervision. Thank you for always challenging me to see the bigger picture and to always ask the question “so what?”. To my unofficial co-supervisor, Dr Daléne Vosloo, I greatly appreciate all your support in the laboratory and for always keeping an open door policy.

Thank you to Dr Paula Sommer for the use of laboratory equipment and consumables. To my friends and colleagues from the Sommer lab your time and assistance is greatly appreciated. A big thank you to Roxanne Wheeler and Nimisha Singh for freely sharing their expertise and experience. Your lab visits were also tremendously appreciated. To Kimberly Pistorius, a very special thank you to you for keeping me focused and for being my very entertaining lab sister! All of your assistance and extensive troubleshooting knowledge is hugely appreciated.

The technical assistance of Marine Sciences Unit manager, Mr Roy Jackson, is also acknowledged, along with that of Mrs Neervana Rambaran for the loaning of equipment and her general interest and support. The specimen contributions from HIK and Wild Coast Abalone farms are appreciatively acknowledged. Acknowledgements also go to uShaka Marine World for the temporary housing and maintenance of specimens.

To my friends, thank you for bringing balance to my days. Thank you for the times spent engaged in stimulating, non-work related discussions at the precious lunch table, they were a welcomed break.

Lastly, my sincere gratitude to my family. Thank you for your support through all my years of study. I appreciate your patience and positivity, and for reminding me of the truly important things in life.

Above all, I would like to thank the Almighty, without Whom I would not have made it this far.

This work was funded in part by the College of Agriculture, Engineering and Science, of the University of KwaZulu-Natal, South Africa (for the first year of study) and by the South African National Research Foundation (for the second year of study).

1. INTRODUCTION

The commercial cultivation of abalone has seen a dramatic increase worldwide with production exceeding that of abalone fisheries (Cook and Gordon, 2010). The decline in the numbers of wild abalone fished has been driven by various factors with over-exploitation accounting for a major part of this decline (Troell *et al.*, 2006). Cultivation thus offers a means to reduce pressures on natural stocks of abalone, a delicacy which is in high demand. The cultivation of abalone in South Africa has grown rapidly such that the country is now the largest producer of abalone outside of Asia (Troell *et al.*, 2006).

Of the six species of *Haliotis* occurring along the South African coastline only *Haliotis midae* is of commercial value (Sales and Britz, 2001). This species exists at a gradient of temperatures ranging from 12/13°C to 21°C (Sales and Britz, 2001). This is due to the two currents which converge along the South African coast: the cold Benguela on the West coast and the warmer Agulhas on the East coast (Branch *et al.*, 1981) (Figure 1.1.). Animals along the East coast are thus living at the edge of their upper thermal limits as the optimal range for the physiology of juvenile *H. midae* is 12°C to 20°C (Sales and Britz, 2001). A decadal increase of 0.5°C has been observed on the East coast for the period 1982 – 2009, while a decrease of 0.55°C per decade has been noted on the West coast for the same period (Rouault *et al.*, 2010). It is possible that this gradient of temperature along the coastline may be widened by global climate change, an occurrence which is likely to have implications for the distribution of species in this area. Global climate change has been seen to have already caused shifts in the ranges of some marine species to regions which are historically cooler than the regions of origin (Somero, 1995; Harley *et al.*, 2006).

In a study by Perry *et al.* (2005) in which the distribution patterns of 36 North Sea fishes were monitored from 1977 to 2001, it was found that two thirds of the species surveyed shifted in latitude in response to warming. The majority of these fish migrated northwards towards lower sea temperatures, covering distances of between 48 km and 403 km (Perry *et al.*, 2005).

In 45 intertidal invertebrate species occupying the Californian coast the abundance of the southern and northern communities was noted to have been altered when comparing the abundance taken between 1931 – 1933 and 1993 – 1994. The increase in mean annual sea temperatures by 0.75°C during this period resulted in eight out of the nine southern species increasing in abundance while five of the eight northern species were observed to decrease in abundance (Barry *et al.*, 1995).

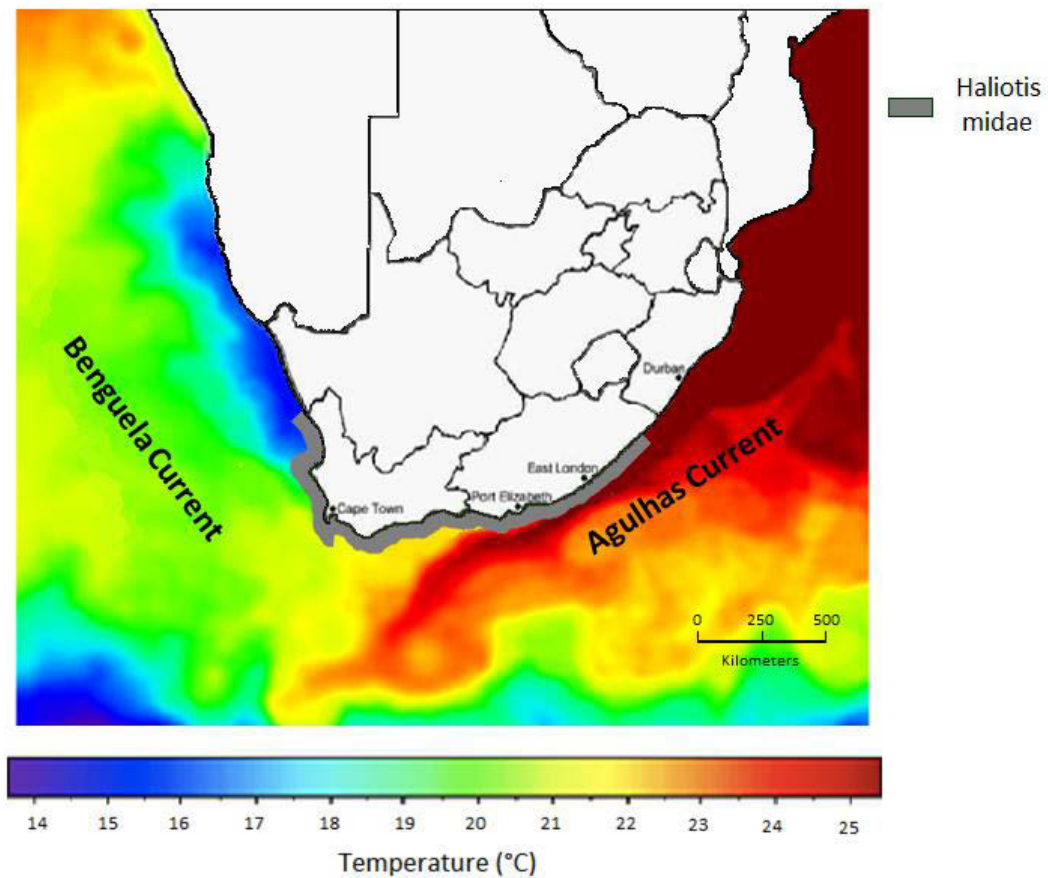


Figure 1.1: A map of the South African coastline illustrating the convergence of the Benguela and Agulhas Currents, along with the estimated species distribution of *Haliotis midae* (adapted from Proudfoot (2007) and <http://www.seos-project.eu/modules/oceancurrents/oceancurrents-c04-p05.html>).

Biogeographic range shifts occur as a result of the inability of the phenotype of the organisms to make sufficient changes for adaptation (Pörtner *et al.*, 2004). The occurrence of these shifts in distribution may have profound implications on the commercial production of abalone, as regional extinctions may result especially for farms placed on the warmer East coast. Summer mortalities have already been noted at the East coast based farms, specifically the adult size classes (R.B. Clarke¹ pers. comm., 2013). This may be due to the higher thermal conditions experienced along the East coast where animals experience temperatures ranging from 17°C to 19°C for majority of the year, while animals on the West coast are exposed mostly to temperatures between 14°C and 16°C (Figure 1.2.).

¹ Mr R.B. Clark, Wild Coast Abalone (Pty) Ltd., Farm 259 East London, Eastern Cape, 5272, South Africa.

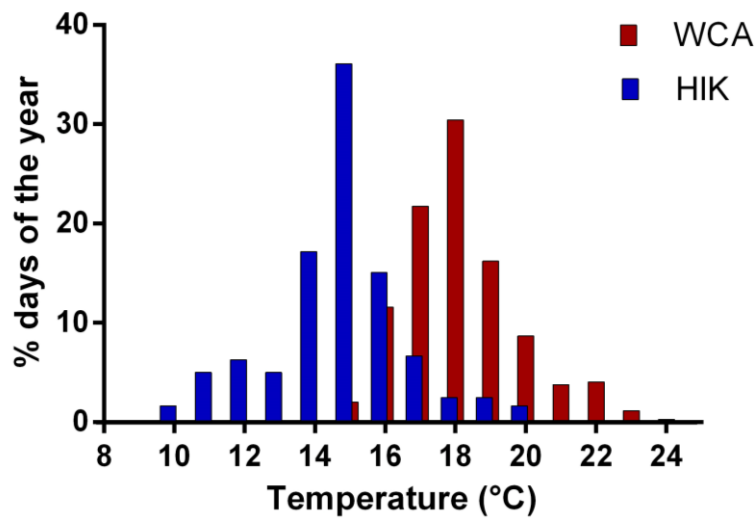


Figure 1.2: Annual temperature profiles of a West coast based abalone farm (HIK) versus that of an East coast based farm (WCA). (From Vosloo A., 2013; unpublished).

1.1. Thermal Stress in Marine Organisms

Exposure to high temperatures has been found to be stressful to marine organisms, but many of the past studies focused on exposing animals to single extreme heat shocks or exposure to extreme but constant temperatures. A study by Vosloo and Vosloo (2010), revealed that abalone exposed to high temperatures within their optimal range for growth (viz. 16°C, 19°C and 22°C) were able to adapt to these thermal regimes provided that temperatures were kept constant. In this case animals were able to adjust to the altered temperatures by altering their biological processes to meet their new physiological requirements. Whether this scenario is the case in the natural environment seems unlikely due to the lack of correspondence between thermal treatments in the laboratory and temperature patterns seen in nature (Figure 1.3.). It is important that studies replicate temperatures (and patterns) that would be experienced in the natural environment in order to better predict how animals will cope with changes to the climate. A number of studies have attempted to do just this.

In a study by Anestis *et al.* (2007), the thermal response of the mussel *Mytilus galloprovincialis* was assessed at various levels of biological organization. In this study animals were exposed to fluctuating temperatures where the ambient temperature (18°C) was raised linearly to 20°C, 24°C, 26°C, 28°C and 30°C for each treatment. *M. galloprovincialis* was found to initiate a thermal response across all levels of biological organization. These responses were found to be indicative of a shift from aerobic to anaerobic metabolism and provided evidence that these

organisms may be living close to the edge of their thermal limits for physiological functioning (Anestis *et al.*, 2007). This study, although being a closer representation of environmental conditions, still depicts only half of the story when it comes to the thermal responses of organisms. This is because the focus is on the increase of temperatures but does not also track how animals will respond when temperatures again decline as will be the case in nature.

High temperatures, or temperature increases alone, do not provide a full demonstration of the conditions during South African summers as they are also characterized by great temperature variability (Figure 1.3.). This variability occurs not only on a monthly or weekly basis but also during the course of a single day, and it is this variability which may potentially be a source of significant thermal stress (Vosloo and Vosloo, 2010).

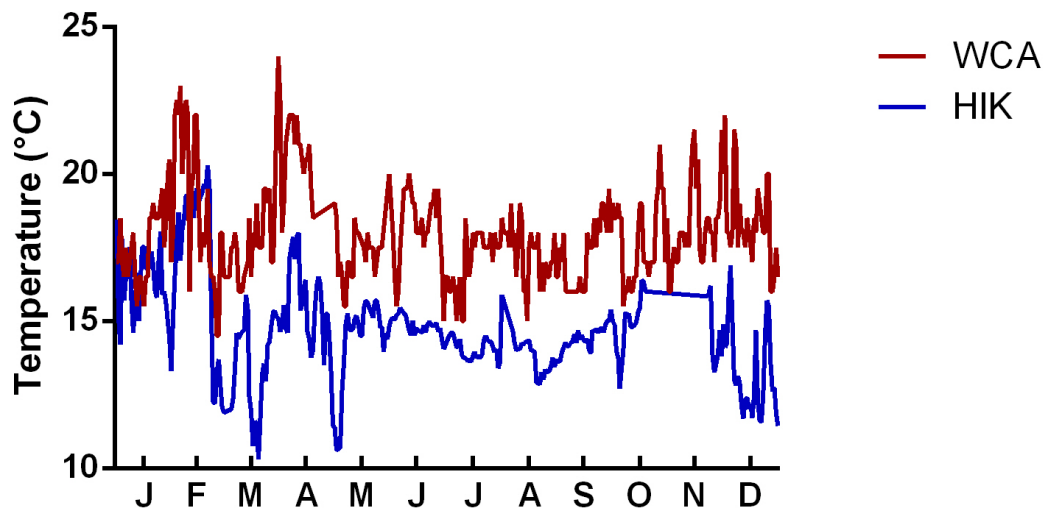


Figure 1.3: Mean daily temperatures experienced at a West coast (HIK) and an East coast (WCA) based farm, taken over a 5 year period (From Vosloo A., 2013; unpublished).

The killifish *Austrofundulus limnaeus* when exposed to high constant temperatures also initiated a stress response (Podrabsky and Somero, 2004) as seen in the previous two studies. In this study however, *A. limnaeus* was also exposed to fluctuating temperatures which involved an increase followed by a decrease in temperature during the course of a single day. This treatment also resulted in the initiation of the thermal stress response but via different mechanisms resulting in the differential expression of certain genes, most notably those for cell growth and proliferation and those encoding molecular chaperones.

Whether these changes in gene expression translate to the level of the whole organism and confer the ability to better adapt to thermal stresses remains unclear. The response of an organism at various levels of organization, upon exposure to fluctuating temperature, thus needs to be investigated to assess if animals will be able to survive future changes in climate.

1.2. The Effects of Temperature on Aerobic Performance

Changes in temperature which are seen to affect populations manifest as a result of the temperature effects on the individuals of a population which have been affected at an organismal level. Thermal adaptation is constrained by the ability of an organism to provide oxygen for all of its physiological processes (Pörtner and Knust, 2007). The range in which an organism most efficiently supplies oxygen for aerobic functioning is referred to as its thermal window (Pörtner and Farrell, 2008). The centre of this window represents the optimum temperature with points further on from this indicating temperatures where aerobic scope becomes limited (Figure 1.4.). The reduction in performance is first apparent at pejus temperatures (T_p) (blue bands) where oxygen delivery is limited such that hypoxemia results (Pörtner and Farrell, 2008). At this stage organisms revert to metabolic depression to cope with these temperatures. Thereafter the critical temperatures (T_c) (green bands) are reached where aerobic metabolism can no longer be sustained, and stress protection mechanisms are initiated to cope with the damage associated with temperature extremes (Pörtner and Farrell, 2008). Beyond these temperatures, thermal tolerance is significantly reduced or lost resulting in denaturation of structural proteins and the loss of molecular function (Pörtner and Farrell, 2008).

The onset of processes intended to assist in tolerance along this thermal window may be used as indicators of an organism's performance in response to thermal challenges. In this study comparing the responses of two different populations of *H. midae* may provide understanding into how some organisms are able to survive the variability of South African summers while others appear to have difficulty in doing so. At the pejus temperatures (T_p) aerobic performance is first limited and one would expect this change to be reflected by the rate of oxygen consumption.

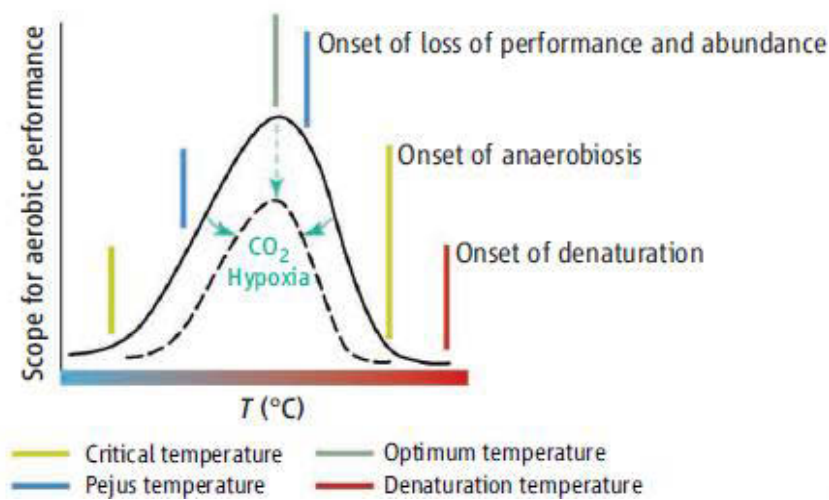


Figure 1.4: The thermal window of aquatic animals as set by scope of aerobic performance. The peak of the curve displays the optimum temperature for aerobic performance (grey band) with points further from this indicating pejus temperatures (T_p) (blue bands), followed by critical temperatures (T_c) (green bands), and lastly denaturation temperatures (red band). Adapted from Pörtner and Farrell (2008).

Measuring oxygen consumption gives an indication of the metabolic rate of an organism (Vosloo *et al.*, 2012) and can thus be used to assess the onset of thermal limitation. Organisms which are better able to maintain the oxygen supply during times of thermal stress are those with the capacity to adapt to these thermal challenges (Pörtner and Knust, 2007). Organisms with wider aerobic ranges will thus be those more likely to survive environments which are warming due to global climate change. Limitations in the thermal response of an animal, which are first manifested by limitations in oxygen delivery, occur at the T_p (Figure 1.4.) (Pörtner and Knust, 2007). At these temperatures the initial response of the organism is to increase oxygen delivery to meet the demand, a process which is energetically costly both to initiate and to maintain (Vosloo *et al.*, 2012). Increasing the oxygen consumption rate also heightens the risk of electron leakage in the electron transport chain (ETC) meaning that animals become more susceptible to accumulating reactive oxygen species (ROS) (Vosloo *et al.*, 2012). ROS are present in cells as a product of normal metabolism but are maintained at low levels by the antioxidant systems of the organism (Scandalios, 2005). Molecular damage arises when ROS accumulate leading to oxidative stress either as a result of their increased production due to an external stress (e.g. thermal stress) or as a result of a depletion in the antioxidant capacity of the organism (Figure 1.5.) or both (Scandalios, 2005).

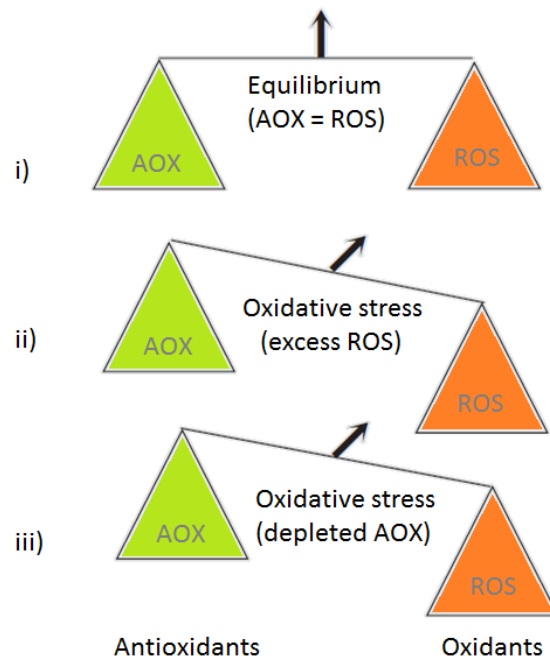


Figure 1.5: Oxidative stress – i) Optimal conditions in a biological system where antioxidants (AOX) are in balance with the amount of reactive oxygen species (ROS) produced. ii) Unbalanced system where excess ROS production results in oxidative stress. iii) Unbalanced system where antioxidant depletion leads to oxidative stress. Adapted from Scandalios (2005).

1.3. The Consequences of Elevated Metabolic Rates

One way in which ROS damage can manifest in proteins is through carbonylation, a process which renders proteins non-functional (Nyström, 2005; Vosloo *et al.*, 2012). Prolonged exposures to the T_p therefore have implications for cultured abalone, by impeding growth rates and thus productivity, and on natural abalone stocks, the survival of which may be affected.

Limitations in oxygen delivery are reached at lower temperatures in the case of larger sized animals (i.e. adults) when compared to smaller sized animals (Pörtner and Farrell, 2008). This is because of the narrowing of thermal windows with age, a phenomenon which may explain the higher incidences of adult mortalities observed on abalone farms, especially those occupying the East coast, during the summer months. Measuring the oxygen consumption rates of thermally stressed abalone from different biogeographical ranges may thus be employed as a method for detecting limitations in thermal responses early on, a method which may provide the aquaculture industry with a range of temperatures that if exceeded countermeasures should be taken to avoid the worsening of the physiological state of the animals.

Once the respiratory mechanisms have been impaired, a stage where the oxygen demand exceeds the capacity of the organism to deliver it, a shift to anaerobic metabolism is initiated (Pörtner and Knust, 2007; Pörtner and Farrell, 2008). The initiation of anaerobiosis thus indicates that critical temperatures (T_c) have been reached and that thermal resistance has been further impacted upon.

1.4. Anaerobic Metabolism

Of the many metabolites that molluscs are known to produce in response to anaerobic metabolism, only D-lactate and tauropine are accumulated by the Haliotids (Gäde, 1988; O'Omolo *et al.*, 2003). The principal enzymes used are D-lactate dehydrogenase (D-LDH) and tauropine dehydrogenase (TDH), which accumulate in the foot muscle and shell adductor muscle respectively (Figure 1.6.) (Gäde, 1988). The use of both of these reductases for indicating anaerobic stress is preferred to using glycogen reserves as these reserves are too unstable for analysis (Wells and Baldwin, 1995). D-lactate was assessed as the only end product of anaerobic metabolism in this study however, as some contention still exists as to the exact biological role of tauropine (Wells and Baldwin, 1995).

The switch to anaerobic glycolysis is useful in maintaining metabolism for short periods when oxygen is limited (Wells and Baldwin, 1995). Prolonged reliance on anaerobic metabolism however, leads to the accumulation of destructive by-products (i.e. organic acids such as D-lactate) which may be harmful to organisms as they result in pH imbalances, but also affect meat quality which may negatively impact the aquaculture industry (Livingstone, 1991; O'Omolo *et al.*, 2003). Utilisation of anaerobic metabolism also requires the initiation of the organism's buffering system (to reduce acidity), a process which also raises the energy expended by the organism (Livingstone, 1991).

Despite the reduced susceptibility of adult abalone to D-lactate accumulation (Wells and Baldwin, 1995), it must still be ensured that levels of this end product are kept to a minimum to ensure they do not reach levels which are toxic for the survival of juvenile abalone preventing them from progressing to later life stages.

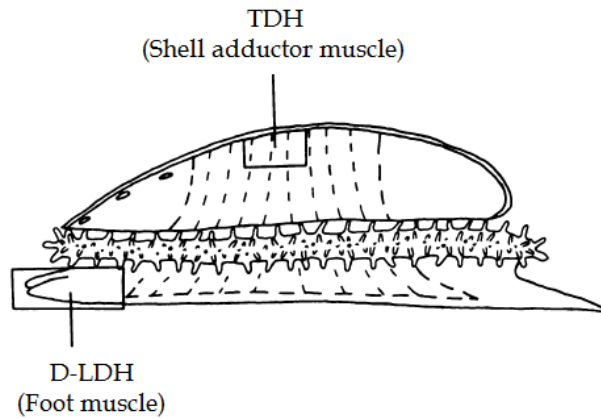


Figure 1.6: Sites of tissue sampling (indicated by boxes) where the enzyme activities for D-lactate dehydrogenase (D-LDH) and taupine dehydrogenase (TDH) can be measured. Adapted from Gäde (1988).

Additional measures which are associated with a decline in aerobic function as a result of thermal challenge, and which were employed in this study include ammonia excretion and the use of the oxygen: nitrogen (O:N) ratio.

1.5. The End-Products of Protein Metabolism and Toxicity

The end-products of protein catabolism are eliminated by *H. midae*, as with other marine molluscs, as ammonia (Lyon, 1995). Ammonia exists in two forms, unionised ammonia which is the toxic form and ionised ammonia, the non-toxic form (Lyon, 1995; Reddy-Lopata *et al.*, 2006). The proportion of both these forms in water is determined by pH, salinity and temperature. Increases in temperature result in the elevated levels of unionised ammonia due to the rise in ammonium ion (NH_4^+) hydrolysis (Lyon, 1995). Temperature increases also contribute to ammonia accumulation in stressed animals particularly due to their increased sensitivity as a result of the stress (Randall and Tsui, 2002). These stressed animals have increased rates of protein catabolism which also leads to further increases in the ammonia levels (Randall and Tsui, 2002). Ammonia toxicity leads to alterations in the gill physiology, because of the ease with which unionised ammonia is able to diffuse across the membranes of gills, leading eventually to death through the lack of adequate oxygen supply (Lyon, 1995). Chronic exposure to sub-lethal doses of ammonia however, results in the reduction of growth rates (Reddy-Lopata *et al.*, 2006). Growth is impacted upon as a result of the energy invested into counteracting the accumulation of ammonia (Reddy-Lopata *et al.*, 2006). This is possibly due

to the temporal compartmentalization of metabolic processes (which may produce ROS) from those which are involved in cell growth and proliferation as these require the molecular stability (Tomanek, 2010).

The effects of ammonia accumulation, as is the case with D-lactate, are more pronounced in smaller abalone (Reddy-Lopata *et al.*, 2006). This means that situations where ammonia levels are elevated for prolonged periods should be avoided to ensure the growth of juvenile abalone to maturity (Reddy-Lopata *et al.*, 2006).

This increase in protein catabolism occurring in stressed animals may be detected by the use of the O:N ratio. The O:N ratio is a ratio of oxygen consumption and nitrogen excretion, and is useful in indicating the type of metabolic substrate being utilised by an organism (Mayzaud and Conover, 1988). High values (i.e. around 50) indicate carbohydrate and/ or lipid metabolism, while low values (below 30) indicate a reliance on protein metabolism, where extremely low values (i.e. 7) indicate a complete reliance on protein metabolism (Vosloo *et al.*, 2012).

A heavy reliance on proteins for metabolic processes is harmful to the growth of abalone as proteins are the emergency stores, the depletion of which may result in the utilisation of structural proteins (Vosloo *et al.*, 2012). The ability of an organism to sustain an O:N ratio in the healthy range (around 50) therefore depends not only on the duration of stress but also the body composition of the organism, with animals which contain more lipid stores being able to survive better (Mayzaud and Conover, 1988). This is particularly concerning for the abalone industry as abalone have low lipid levels in their tissues meaning that very little can be utilised as a substrate (Laas and Vosloo, 2010; Vosloo and Vosloo, 2010). The analysis of ammonia concentrations and the O:N ratio, a method more appropriate than using body constituents to assess substrate utilisation (Mayzaud and Conover, 1988), may therefore provide an indicator of situations where aerobic scope is limited past the T_c such that protective responses can longer be utilised (Pörtner, 2008).

1.6. The Stabilization and Destabilization of the Protein Pool

Beyond the T_c , denaturation temperatures (T_d) are reached (Figure 1.4.), where cellular repair processes are initiated to combat denaturation (Pörtner, 2008). This repair response utilises heat shock proteins (Hsp's) and antioxidants (Pörtner, 2008). Under normal conditions, Hsp's function as molecular chaperones involved in the initial folding of nascent polypeptides, the

refolding of denatured proteins and also in preventing the formation of protein aggregations (Snyder *et al.*, 2001; Sørensen *et al.*, 2003). During stressful conditions the induction of Hsp's is increased by the heightened need for a molecular chaperone to stabilize the protein pool (Buckley *et al.*, 2001; Sørensen *et al.*, 2003).

The class of Hsp used in this study was Hsp70; the largest, best studied and most conserved of the Hsp's (Sanders, 1993; Mukhopadhyay *et al.*, 2003). Not only is its induction increased by environmental disturbances, but it has been found to be the most responsive to thermal stress (Lewis *et al.*, 1999). For activation, the transcription factor heat shock factor 1 (HSF1) trimerizes upon being released by Hsp70 (Figure 1.7.) (Hofmann, 1999; Tomanek and Somero, 2002). Once trimerized HSF1 activates the *hsp70* genes by binding to the heat shock element (HSE), which then results in the transcription of Hsp70 mRNA followed by its translation into Hsp70 proteins (Hofmann, 1999; Tomanek and Somero, 2002).

Hsp70 has also been implicated in promoting cell survival by being anti-apoptotic (Garrido *et al.*, 2001). This property suggests that animals with efficient protein repair responses may have the potential to adapt to future thermal challenges, as the heat shock response (HSR) is implicated in setting the thermal limits for the physiology of an organism (Tomanek, 2008).

Because increased levels of Hsp's are not indicators of permanent protein damage (Hofmann and Somero, 1995), additional methods may be employed to assess protein denaturation. The introduction of carbonyl groups (i.e. carbonylation) into the side chains of proteins is an irreversible phenomenon (Nyström, 2005). Once carbonylated, proteins are no longer functional due to conformational alterations, but are also unable to be proteolytically degraded (by the ubiquitin-proteasome pathway) in cases where the oxidation of side chains is extensive (Nyström, 2005).

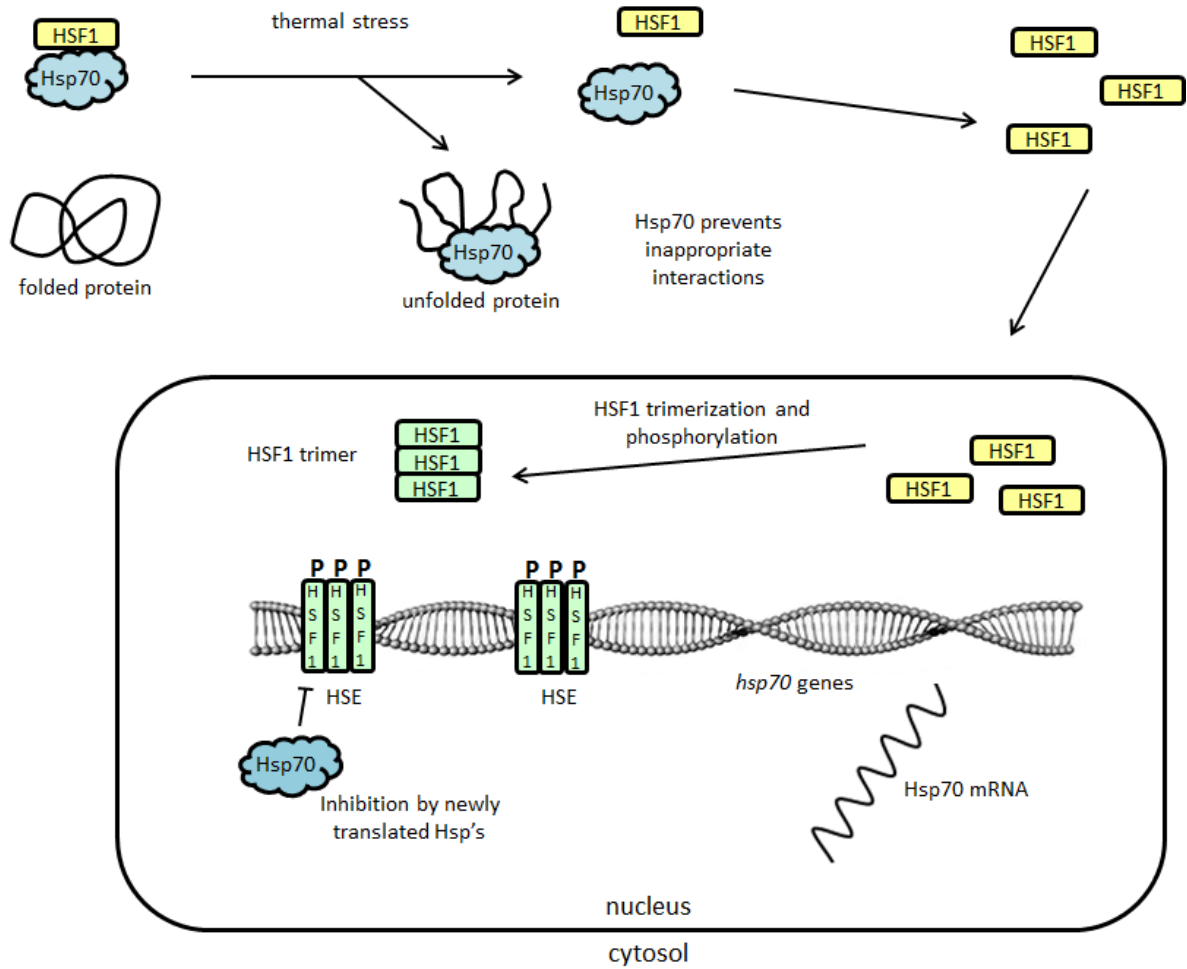


Figure 1.7: The model for the activation of *hsp70* genes and the production of Hsp proteins in response to thermal stress denatured proteins. Adapted from Tomanek and Somero (2002).

If these carbonylated proteins are not degraded by proteases they accumulate in the cell and may become cytotoxic. Over accumulation of carbonylated proteins may thus be regarded as an indicator of imminent cell death, and was a measure that was utilized in this study. Carbonylation, which may be generated by four pathways (Figure 1.8.), may also be used to indicate situations where the Hsp response of an organism was insufficient to combat the thermal stress experienced, and as mentioned is associated with ROS production (Vosloo *et al.*, 2012).

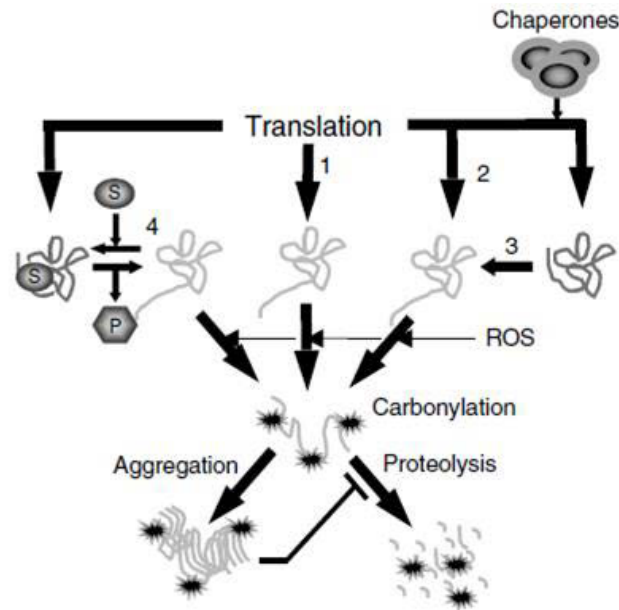


Figure 1.8: Pathways that can generate carbonylation-prone protein species: 1) irregular protein production due to errors in translation, 2) irregular protein conformations as a result of defective chaperones, 3) abnormalities in protein conformations due to denaturing stresses, and 4) the hypothetical formation of carbonyls on idle enzymes which are put at risk as a result of inactivity. Once formed carbonylated proteins form aggregates which appear to inhibit proteolysis. Taken from Nyström (2005).

1.7. Aims and Objectives

In this study, abalone from different biogeographic ranges (i.e. West versus East coasts) were exposed to fluctuating temperatures to assess the variation in their thermal responses and elucidate the mechanisms responsible for conferring thermal resistance to the Western population of *H. midae*. The aim was to elucidate the mechanisms responsible for the thermal sensitivity experienced by abalone in general. It is predicted that animals from the East coast will show greater limitations in the physiological responses to stress specifically during the more challenging summer months, possibly due to occupying a biogeographical region where they are close to their upper thermal limit (Somero, 2005) and because of the greater variability in the temperatures experienced during this period on the East coast (Vosloo and Vosloo, 2010).

The objectives were to use biological processes, at various levels of organization, which occur at essential points along the thermal window of aerobic performance for aquatic animals. Oxygen consumption, nitrogen excretion and the O:N ratio were determined at the organismal level. Oxygen consumption and O:N ratio were employed as both are indicators of metabolic condition (Mayzaud and Conover, 1988; Vosloo *et al.*, 2012) where increased oxygen

consumption would indicate T_p 's (i.e. no longer optimal conditions) and decreases in the O:N ratio would be indicative of a switch to protein catabolism. Nitrogen excretion on the other hand, was used not only as an indicator of a loss in performance but also to give an indication of the amounts of protein waste being produced (Wright, 1995). D-lactate production was assessed at the biochemical level. This was used to indicate a shift to anaerobic metabolism as is the case when critical temperatures are reached (Pörtner and Farrell, 2008).

The presence of Hsp70 was determined at the proteomic and transcriptomic levels in order to provide a better understanding of the mechanisms responsible for thermal sensitivity or resistance in abalone. It is important to include the transcriptomic activation of *hsp*'s as alterations of major cellular actions are initiated at this level (Bustin, 2000). It is also imperative to couple transcriptomic and proteomic analyses as this not only provides a broader understanding of the processes relating to thermal adaptation but also because the changes observed at the transcriptomic level may not always be translated to higher levels of organization (i.e. in the form of proteins) (Podrabsky and Somero, 2004).

The accumulation of carbonyls was also quantified at the proteomic level. This was due to the fact that Hsp's alone are unable to indicate whether proteins have incurred any permanent damage as would likely occur at denaturation temperatures (Hofmann and Somero, 1995; Pörtner and Farrell, 2008)

It is thus hypothesized that abalone exposed to greater amounts of stress, in the form of larger temperature fluctuations, will initially elicit greater protective responses in proportion to the amount of thermal stress experienced. This is expected to continue until (or if) adaptation to new conditions occurs. Abalone occupying various biogeographic ranges will have differing responses to thermal stress, where cold-adapted animals (West coast animals) will be better equipped to handle temperature variation in comparison to the warm-adapted counterparts. In future, these adaptations may restrict the occurrence of *H. midae* to certain regions along the South African coastline, it is thus imperative that mechanisms responsible for adaptation be elucidated so that the abalone aquaculture industry can make the necessary changes (e.g. to farm infrastructure) before regional temperatures are worsened by global climate change.

2. MATERIALS AND METHODS

2.1. Collection and Acclimation

Eighty abalone were sourced from HIK abalone and Wild Coast Abalone (WCA) farms respectively. Abalone were transported overnight, on ice, and were then housed at the Marine Science Unit (MSU) at the University of KwaZulu-Natal (Westville campus), South Africa. Once at the MSU they were allowed to acclimate for at least seven days at 16°C before exposures were initiated. Abalone were kept in 100 L tanks in a 1 000 L capacity recirculating system with a flow rate of 3000 L hr⁻¹ in which temperature was regulated using a 1800 kW chiller (Hailea, HC-2200BH). Filtered seawater (10 µm) was obtained from uShaka Marine World and allowed for a 10% water change weekly.

Abalone were kept at a stocking density of 40 animals per 100 L tank, each of which was provided with additional aeration in order to maintain the oxygen content of the seawater. Abalone were fed formulated feed (Abfeed®) twice weekly (0.01 g per 1 g animal) except on days immediately prior to sampling which was done on days 1, 3, 7 and 14 of exposure. Water quality was measured daily to ensure consistent holding conditions. Temperature (°C), conductivity (mS cm⁻¹), salinity (‰), dissolved oxygen (mg L⁻¹) and pH were measured using the YSI 556 Multi-parameter system (YSI Inc., USA). Water samples were collected three times a week from which total ammonia was measured using a modified phenol-hypochlorite method (outlined in section 2.4. below). Total ammonia nitrogen (TAN) was converted into free ammonia nitrogen (FAN), using the algorithm below, and the average values for the water quality parameters measured are listed thereafter (Table 2.1.).

$$\text{NH}_3 (\text{Free}) = \text{TAN} \times \left(1 + \frac{10^{-\text{pH}}}{10^{-\left(0.09018 + \frac{2729.92}{\text{T(K)}}\right)}} \right)^{-1}$$

Where: NH₃(Free) = FAN concentration (mg L⁻¹)

TAN = total ammonia nitrogen concentration (mg L⁻¹)

T(K) = temperature in Kelvin

Table 2.1: The average water quality values (shown with standard error) measured during the acclimation period as well as for the control tanks for the duration of exposures. Minimum and maximum water quality values given in brackets.

	Temperature (°C)	Salinity (‰)	Dissolved oxygen (mg L ⁻¹)	pH	FAN (µg L ⁻¹)
West Coast	15.9 ± 1.4 (14.1 – 16.9)	33.8 ± 0.4 (33.5 – 34.7)	7.6 ± 0.4 (7.2 – 8.0)	8.2 ± 0.1 (8.1 – 8.3)	2.4 ± 1.6 (1.2 – 4.3)
East Coast	15.6 ± 1.0 (14.7 – 16.6)	34.2 ± 0.5 (51.3 – 52.7)	7.4 ± 1.0 (6.3 – 8.4)	7.9 ± 0.3 (7.7 – 8.2)	0.7 ± 1.1 (0.3 – 2.5)

2.2. Exposure and Sampling

Exposures lasted for the duration of two weeks in each case with the first set of exposures, using animals obtained only from HIK, being carried out during December 2012 and the second set of exposures, using animals from WCA, being carried out during June 2013. The control animals were maintained at 16°C, while the experimental animals were exposed to fluctuating temperatures. A temperature of 16°C was selected for the control animals as this value falls at the midpoint of the optimal thermal range (12°C - 20°C) for the functioning of juvenile *H. midae* (Sales and Britz, 2001). This was applicable to the study as the animals selected were of the pre-adult stage and of weight 63.2±8.6 g and shell length 6.7±0.65 cm. The fluctuating temperatures used for the exposures was selected on the basis of being more representative of the patterns experienced on the land based holding systems (Vosloo and Vosloo, 2010). The experimental animals were divided into two groups; the first exposed to a temperature regime in which the minimum and maximum temperatures were 2°C less than and greater than (16°C±2) that of the control; and the second group had a variation of 4°C (16°C±4) above and below that of the control group. The fluctuations that the first group was exposed to thus oscillated from 14°C to 18°C daily, while the fluctuations of the second group oscillated from 12°C to 20°C (Figure 2.1.). All groups of abalone (control and experimental) were thus exposed to a mean temperature of 16°C. Temperatures were manipulated by the addition of heated or chilled seawater, directly to treatment tanks, to achieve a change in temperature at a rate of 2°C per hour.

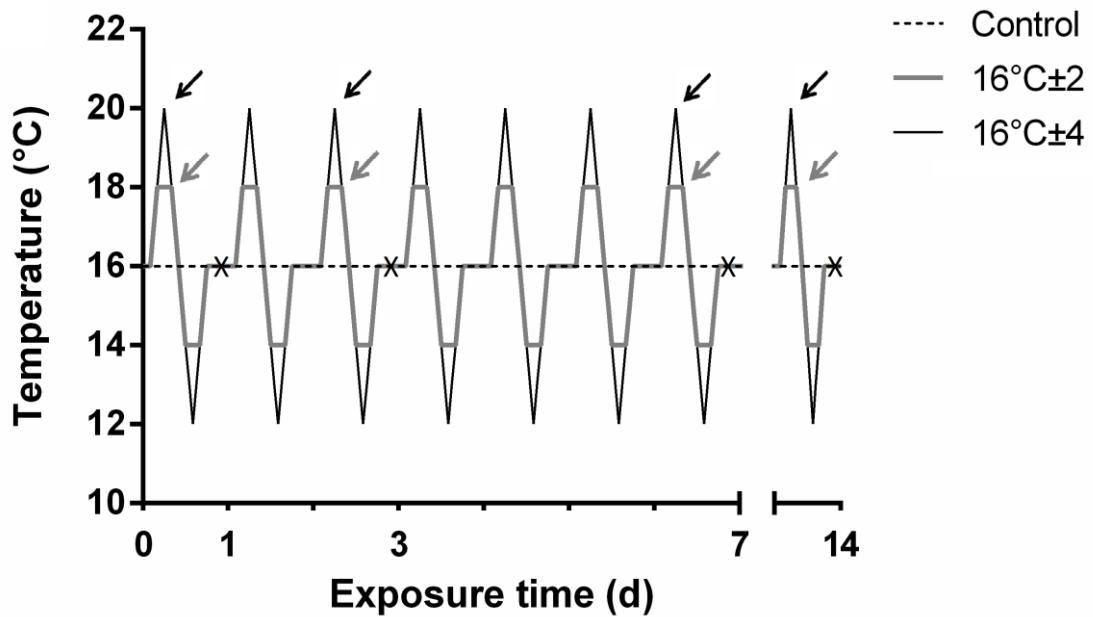


Figure 2.1: Temperature fluctuations as experienced by abalone exposed to the two experimental temperature regimes. Animals belonging to experimental group $16^{\circ}\text{C}\pm 2$ were exposed to a minimum temperature of 14°C and a maximum temperature of 18°C ; while experimental group $16^{\circ}\text{C}\pm 4$ was exposed to a minimum temperature of 12°C and a maximum of 20°C . Sampling occurred prior to the commencement of temperature spikes (indicated by crosses) while oxygen consumption readings and ammonia samples were taken at the highest temperature that animals were exposed to in each experimental group (indicated by arrows).

Animals were sacrificed on days 1, 3, 7 and 14 after the high and low temperature spikes had been reached (Figure 2.1). Paired oxygen consumption and ammonia excretion measurements were also obtained on these days. Oxygen consumption and ammonia excretion measurements were collected at the maximum temperatures experienced by the treatment groups i.e. 18°C for the $16^{\circ}\text{C}\pm 2$ group and 20°C for the $16^{\circ}\text{C}\pm 4$ group (indicated by arrows on Figure 2.1). After shucking foot tissue was collected along with haemolymph which would be used for biochemical analyses. Tissue samples, once cut into smaller pieces, were snap frozen in liquid nitrogen and later transported to the laboratory for storage at -80°C until further use.

2.3. Oxygen Consumption Rates

Oxygen consumption measurements were taken using one closed respiration chamber per animal where oxygen electrodes were used to measure the decrease in the partial oxygen pressure (PO_2) of the water in the chamber. The chambers (350 mL glass jars) were first flushed with seawater of a known PO_2 , which was measured as PO_2 (1) before abalone were placed in and the chambers then closed. The PO_2 in the chambers was then allowed to decrease over a period of 10 minutes (after abalone had been placed in the jars) before the PO_2 was again measured, this being PO_2 (2). This process was then repeated to yield 6 biological repeats in total.

The difference in PO_2 , along with the masses of the animals (recorded prior to the measurement of the PO_2), was then used for the calculation of the specific oxygen consumption (MO_2), calculated in $\mu\text{mol kg}^{-1} \text{min}^{-1}$, as outlined by Van Aardt and Booyesen (2004). The respiration rates of the animals kept in the tank maintained at constant temperature (16°C) were used as the control rates.

2.4. Ammonia Excretion Rates

Water samples of 5 mL each were collected in triplicate on the same days that oxygen consumption was measured. These samples were frozen and later analyzed using the phenol-hypochlorite method as described by Solórzano (1969). This method required that 0.2 mL of phenol solution (Appendix A.1.1.), 0.2 mL of nitroprusside solution (Appendix A.1.2.) and 0.5 mL of oxidizing solution (Appendix A.1.4.) be added to 5 mL of incubation medium (i.e. samples, standards and blanks) with adequate mixing following the addition of each solution. Samples were then incubated in the dark at room temperature for 2 hours to allow for color development. The absorbance of these samples was then read spectrophotometrically (PowerWave XS) at 640 nm after 200 μL of each sample was transferred to a microplate. The concentration of the samples was determined by extrapolation off a standard curve generated using a serial dilution of standard master solution (Appendix A.1.5.) of known concentration. The rates of ammonia excreted were then calculated as $\mu\text{mol kg}^{-1} \text{min}^{-1}$.

2.5. Oxygen: Nitrogen Ratio

The ratio of oxygen consumed versus nitrogen excreted (i.e. O:N ratio) was then calculated as μmol of oxygen consumed to μmol of nitrogen excreted using the values obtained from the oxygen consumption and ammonia excretion experiments.

The oxygen consumption values were multiplied by two, to account for the molecular equivalents of oxygen, and this then divided by the ammonia excretion values. Thus,

$$\frac{(\text{MO}_2 \times 2)}{\text{MNH}_4\text{-N}}$$

O:N ratios were calculated for each individual as oxygen consumption and ammonia excretion rates were simultaneously measured per organism.

2.6. D-Lactate Accumulation

Haemolymph samples were collected on sampling days and were frozen in liquid nitrogen and stored at -80°C for the later analysis of the presence of D-lactate. The enzymatic analysis of D-lactate was performed using a D-lactic Acid Assay kit (Megazyme, Ireland). This kit oxidized D-lactate in a two-step reaction which produced NADH (which is proportional to the amount of D-lactate contained in a sample) that was then quantified via spectrophotometer.

The microplate assay protocol was used where $150 \mu\text{L}$ aliquots of distilled water, $50 \mu\text{L}$ D-glutamate solution, $10 \mu\text{L}$ NAD^+ solution and $20 \mu\text{L}$ D-glutamate-pyruvate transaminase (D-GPT) suspension were added to each well containing $10 \mu\text{L}$ of sample. For the blanks, the volume of sample was removed and replaced with $10 \mu\text{L}$ distilled water. The absorbance was read at 340 nm using a PowerWave™ XS (BioTek Instruments, Inc., USA) following a waiting period of 3 minutes, and the values obtained at this stage representing A_1 . A D-lactate dehydrogenase (D-LDH) suspension ($20 \mu\text{L}$) was then added to the wells and the absorbance again read, after 5 minutes of incubation, to yield the A_2 value. The overall absorbance ($\Delta A_{\text{D-lactate}}$) was then determined by subtracting the absorbance difference ($A_2 - A_1$) of the blanks from that of the samples. The concentration of the samples was calculated using the following equation:

$$c = \frac{V \times \text{MW}}{\epsilon \times d \times v} \times \Delta A_{\text{D-lactate}}, \text{ where } V \text{ is total volume (250 } \mu\text{L), MW the molecular weight of D-lactate, } \epsilon \text{ the extinction co-efficient of}$$

NADH at 340 nm ($6300 \text{ L} \times \text{mol}^{-1} \times \text{cm}^{-1}$), d the light path distance, and v is the sample volume (10 μL).

2.7. Dot Blotting

2.7.1. Protein Extraction

Protein was extracted using the method outlined by Drew *et al.* (2001), with all of the subsequent steps being performed on ice. Lysis buffer (670 μL) containing 32 mmol L^{-1} Tris-HCL (pH 6.8), 2% SDS, 1 $\mu\text{mol L}^{-1}$ PMSF, and 2 $\mu\text{g L}^{-1}$ each of pepstatin, chymostatin and leupeptin was added to approximately 100 mg of muscle tissue. The tissue was roughly cut up in a 2 mL tube before being heated at 100°C using a dry bath incubator (MRC, Israel) for 3 minutes. Thereafter the tissue was disrupted for 7 minutes at an oscillation frequency of 50 Hz (TissueLyser LT, Qiagen, Netherlands). This disruption step was repeated where protein was not sufficiently reduced to small pieces. The resulting homogenate was again boiled for 5 minutes and the lysate then centrifuged at 13 000 $\times g$ for 10 minutes. The supernatant was then collected and the protein within quantified prior to long term storage at -80°C.

2.7.2. Protein Quantification

Total protein quantification was done using the Pierce BCA Protein Assay kit, according to the manufacturer's instructions, where differences in protein concentration were measured as color variations. Briefly, 9 standard solutions of known protein concentration (prepared by serially diluting the 2000 $\mu\text{g} \mu\text{L}^{-1}$ assay standard) were pipetted into a 96-well microplate along with a 1:10 dilution of the sample proteins. Reagents A and B, provided in the BCA Assay kit, were then mixed 50:1 in a reagent reservoir and 200 μL of this mixture (working reagent) aliquoted into each well. The microplate was then incubated at 37°C for 30 minutes and the absorbance of the samples read using a PowerWave™ XS (BioTek, USA). The concentrations of the sample proteins were then determined by extrapolation off a standard curve generated using the concentration and absorption values of the BCA protein standards.

2.7.3. Protein Blotting and Detection

Eighty $\mu\text{g L}^{-1}$ of sample proteins were directly applied onto gridded nitrocellulose membranes. This process was performed slowly to ensure that discrete, circular dots were produced. After the applied proteins were allowed to dry, the membrane was incubated in 1x Blocking buffer (Appendix A.2.1.) for 1 hour, before being exposed to the primary antibody (mouse monoclonal anti-HSP70, 1:500) for 30 minutes at room temperature with gentle agitation using a KS 130 Basic orbital shaker (IKA[®], USA). Primary antibody incubation was then followed by a three-step washing procedure using 1x TBS-T (Appendix A.2.2.). Each washing step was 5 minutes long and was accompanied by agitation on the orbital shaker. Washes were followed by incubation in secondary antibody (horse-radish peroxidase (HRP) conjugated goat anti-mouse IgG, 1:1000) for 30 minutes also at room temperature and with agitation. This incubations step was followed by one 15 minute washes, then two 5 minute washes with 1x TBS-T and lastly a 5 minute wash in 1x TBS buffer.

Visualization of the protein dots was performed using the Immun-Star[™] Chemiluminescence Kit (BioRad, USA), and detection of the light being emitted by the sample as a result of substrate oxidation was done using the ChemiDoc[™] XRS+ (BioRad, USA) imaging system used together with its accompanying software (Image Lab[™]). After imaging membranes were stained using Ponceau S (Appendix A.2.3.) for 10 minutes with agitation. Excess stain was rinsed off the membranes using 1x TBS-T before viewing. Whole protein dots obtained from Ponceau S staining are used for the normalization of Hsp70 intensities.

2.8. Oxidized Protein Assay

2.8.1. Sample Preparation and Total Protein Content Determination

Protein was extracted using the Drew *et al.* (2001) method outlined above and the protein quantified using the BCA Protein Assay Kit (described above). Protein stocks were aliquoted from the extracted protein and stored at -80°C until further use. The 280/260 nm ratios were checked to determine the purity of the protein. All sample proteins had 280/260 ratios that were greater than one indicating sample purity.

2.8.2. Carbonylated Protein Content Assay

A *BioVision* Carbonyl Content Assay Kit (K830-100) (BioVision Inc., USA) was used to detect and quantify the protein carbonyls. From the protein stocks, 10 mg mL⁻¹ of protein was loaded into 1.5 mL centrifuge tubes and used for the assay. To this, 100 µL of DNPH solution was added and then each sample vortexed and incubated at room temperature for 10 minutes. Next, 30 µL of TCA solution was added and the samples again vortexed, placed on ice for 5 minutes and centrifuged at 16 000 x g for 2 minutes. After the removal of the supernatant, the pellet was washed. This was done by adding 500 µL of cold acetone to each sample, vortexing for 30 seconds, incubating at -20°C for 5 minutes and then centrifuging at 16 000 x g for 2 min. The acetone was then removed and the washing procedure repeated. Guanidine (200 µL) was added and the protein resolubilized by vortexing. Resistant proteins were incubated at 60°C for 15 minutes with vortexing after every 5 minutes of incubation. Protein samples (100 µL) were then loaded onto the 96-well microplate provided with the kit and the optical density measured at 375 nm using the PowerWave™ XS (BioTek, USA) microplate reader.

2.8.3. Carbonylated Protein Content Calculation

Before the amount of carbonylated proteins could be calculated, the total protein in each well had to be determined in order for the protein carbonyls to be expressed per mg of total protein. The total protein per well was determined using the BCA assay, as previously described, and the protein concentrations extrapolated from the standard curve generated. The carbonylated protein content was then calculated using the following equations:

$$C = [(OD\ 375\ \text{nm} / 6.364) \times 200] \text{ nmol carbonyl per well}$$

$$P = [\text{protein concentration} \times 40] \text{ } \mu\text{g protein per well}$$

$$CP = (C/P) \times 1000 \times D,$$

where 6.364 is the extinction coefficient (L x mol⁻¹ x cm⁻¹), 1000 is the factor for the conversion of µg to mg and D is the dilution factor used (1:10).

2.9. Conventional Polymerase Chain Reaction (PCR)

2.9.1. RNA Extraction and Integrity Assessment

Total RNA was extracted using the TRI Reagent[®] protocol (Sigma, USA), performed according to the manufacturer's instructions. Briefly, 50 mg of foot muscle tissue was weighed and rinsed in 1x PBS (Appendix A.3.1.) to remove the RNAlater[®] (Sigma, USA). The tissue was then placed in a 2 mL micro-centrifuge tube where 500 μ L of cold TRI Reagent[®] (Sigma, USA) were added. The tissue was minced using dissecting scissors and the micro-centrifuge tube placed in a TissueLyser LT (Qiagen, Netherlands) to allow for homogenization which was facilitated by the addition of a stainless steel beads to the tube. The homogenization occurred for 7 minutes at 50 Hz. Afterward, the sample was allowed to stand at room temperature to allow for the complete dissociation of proteins from nucleic acids and 50 μ L of 1-Bromo-3-chloropropane (Sigma, USA) added. The sample was shaken vigorously for 15 seconds, allowed to stand at room temperature for 10 minutes and then centrifuged at 12000 x g, using the Centrifuge 5418 (Eppendorf, Germany), for 15 minutes also at room temperature. The sample at this point was separated into three phases: a lower red organic phase containing protein, a white interphase containing DNA and an upper colorless phase containing RNA. The colorless upper phase was transferred to a fresh 1.5 mL tube, 250 μ L of isopropanol added and the sample mixed by vortexing. The sample was allowed to stand for 5 – 10 minutes at room temperature before being centrifuged at 12000 x g for 10 minutes at room temperature. The resulting supernatant was then discarded and 500 μ L of 75% ethanol (Appendix A.3.2.) added to the RNA precipitate pelleted at the bottom of the micro-centrifuge tube. The sample was vortexed and then centrifuged at 7500 x g for 5 minutes at room temperature. The supernatant was discarded and the pellet allowed to air dry for 5 – 10 minutes. Thereafter, 30 μ L of nuclease-free water (Promega, USA) were added and the pellet dissolved by pipette mixing. Pellets which were not dissolved by this method were heated at 60°C for 10 minutes and again mixed by pipetting.

The extracted RNA was quantified by UV-spectrophotometer (NanoDrop ND-1000) and integrity assessed, in line with MIQE guidelines (Bustin *et al.*, 2009) (Appendix B.), using an RNA integrity gel electrophoresis protocol. All buffers used for this protocol were made up using DEPC-treated water (Appendix A.3.3.) and all gel casting equipment and laboratory ware treated with 3% hydrogen peroxide overnight to ensure the removal of RNAses.

Samples were prepared by mixing 2 µg of RNA with two volumes of RNA loading buffer (Sigma) and heating at 65°C using a dry bath incubator (MRC, Israel) for 10 min. The samples were then loaded onto a DEPC-treated 1.2% agarose gel (Appendix A.3.4.). A 1 kb DNA ladder (GeneRuler™; ThermoScientific, USA) (4 µL) was also loaded onto the gel which was then electrophoresed in DEPC-treated 1x TBE buffer (Appendix A.3.5.) for 45 minutes at 85 V. The resulting bands were then visualised using the ChemiDoc™ XRS+ Imaging System and accompanying Image Lab™ software (BioRad, USA).

2.9.2. Complementary DNA (cDNA) Synthesis

The extracted RNA was DNase-treated to ensure the removal of DNA contaminants. This was done by PCR cycling 2 µg of RNA together with 1 µL of RQ1 RNase-free DNase (Promega, USA) in 1 µL of RQ1 10x Reaction Buffer (Promega, USA), for 30 min at 37°C. Thereafter, 2 µL of STOP buffer (Promega, USA) was added to the tubes which were then cycled for 10 min at 65°C to terminate the reaction.

Prior to cDNA synthesis total mRNA was synthesised. For this the DNase treated RNA was PCR cycled with 1 µL of Oligo (dT)₁₈ primers (Promega, USA) and 2 µL of dNTPs (Promega, USA). Upon binding of the Oligo (dT)₁₈ primers to the poly-A tails of the mRNA molecules, SuperScript™ III reverse transcriptase (Invitrogen, USA) was used to perform the cDNA synthesis. This was done by PCR cycling the mRNA with 4 µL of 5x First-Strand buffer (Invitrogen, USA), 1 µL of dithiothreitol (DTT) (Invitrogen, USA), 1 µL of RNase OUT buffer (Invitrogen, USA) and 1 µL SuperScript™ III reverse transcriptase (RT); for 1 hour at 50°C, 15 min at 55°C and lastly 5 min at 85°C. Once synthesised, cDNA was either used to perform real-time quantitative PCR (qPCR) or was stored at -80°C until further use.

2.9.3. Conventional PCR

The cDNA obtained from the reverse transcription was used to perform quantitative real-time PCR (qPCR) along with primers for *hsp70* (gene of interest) and *coxIII* (reference gene). Primer sequences (Table 2.2.) were obtained from Vosloo *et al.* (2013) and all primers were synthesized by Inqaba Biotec (South Africa). Primers were reconstituted according to the manufacturer's instructions using Nuclease-free water (Promega, USA) to produce stock solutions of 100mM. Primer solutions were aliquoted and stored at -20°C.

The MyCycler™ Thermal Cycler (BioRad, USA) was used to perform all PCR amplifications. Each reaction consisted of: 12.5 µL of Nuclease-free water (Promega, USA), 2 µL of MgCl₂ (Promega, USA), 2 µL of dNTPs (Promega, USA), 2 µL each of forward and reverse primer (Inqaba Biotec, South Africa), 1 µL of template cDNA and lastly 0.5 µL of *Taq* DNA Polymerase (5 U/µL) (Fermentas, Canada). The PCR cycling conditions consisted of a 10 min denaturation step at 95°C, 40 cycles consisting of 15 sec at 95°C, 25 sec at 60°C and 40 sec at 72°C, with a final extension step of 10 min at 72°C.

Table 2.2: Primer sequence information (Vosloo *et al.*, 2013).

Primer	GenBank Accession number	Sequence (5' - 3')
<i>coxIII</i>	HS981866.1	Fwd: TTCCTAATTGTCTGCCTAGTTCG
		Rev: CGGTTTATTGTTGTTTAAGATCC
<i>hsp70</i>	AM283516.1 FJ12176.1	Fwd: CGGCTGTCCAGGCTGCCATC
		Rev: CACCTCTCGGTGCTGGGGGA

2.9.4. PCR Product Electrophoresis

Following PCR, the products were spun down and electrophoresed on a 1.2% agarose gel (Appendix A.4.1.) to confirm that primers had amplified the desired products. Two µL of 6x DNA loading dye (ThermoScientific, USA) were added to 8 µL of sample, which was then loaded onto the agarose gel. A GeneRuler™ DNA ladder (2 µL) (ThermoScientific, USA) was also loaded onto the gel which was then run in 1x TBE buffer (Appendix A.4.2.) for 45 min at 80 V. Once electrophoresed, the bands were visualized using the ChemiDoc XRS+ and the accompanying Image Lab™ software (BioRad, USA).

2.10. Quantitative Real-Time PCR (qPCR)

The Eco Real-Time PCR System (Illumina, USA) was used to perform all qPCR reactions. Each reaction consisted of 12.5 µL of SYBR® Green JumpStart™ *Taq* ReadyMix™ (Sigma), 10.5 µL of Nuclease-free water (Promega, USA), 1 µL of cDNA and 0.5 µL each of forward and reverse primer. SuperScript™ III RT and template were excluded from qPCR runs to yield no RT (noRT) and no template controls (NTC) respectively.

The qPCR conditions used were as those outline by Vosloo *et al.* (2013) (Figure B.3.1. of Appendix). Briefly, 10 min were allowed at 95°C for polymerase activation. This was followed by 40 cycles consisting of 15 sec at 95°C, 25 sec at 60°C and 40 sec at 72°C to allow for denaturation, annealing and extension. The final step consisted of a 0.5°C increment increase from 60°C to 95°C for 5 sec each for the generation of a melt curve (Figure B.4.1. i. of Appendix). This melt curve was used to ensure that the melting temperature (T_m) expected for the amplification products was obtained and that a single T_m was produced by each reaction.

The C_T values generated by the Eco™ Software (v3.0.16.0) were used to calculate the fold-changes in *hsp70* expression (relative to *coxIII*) using the $2^{-\Delta\Delta CT}$ method (Livak and Schmittgen, 2001) (see Appendix B.5.1.). Statistical analyses were then performed on these relative fold-changes using a total of three biological repeats with two technical repeats for each one.

2.11. Statistical Analyses

Multiple one-way analyses of variance (ANOVAs) were performed comparing the oxygen consumption, nitrogen excretion and O:N ratio of organisms from different treatments (control, 16°C±2 and 16°C±4) over time. These parameters (oxygen consumption, nitrogen excretion and O:N ratio) were also compared across biogeographic region for organisms belonging to the same treatment group. Residuals generated by each ANOVA were tested for normality and homoscedasticity using the one-sample Kolmogorov-Smirnov test and the Levene's test respectively. Where the test for normality was not satisfied (viz. O:N ratio data for West coast animals) an independent-samples Kruskal-Wallis test was used.

Statistical significance was taken at 5% and where significant differences were detected, the Tukey HSD post-hoc analysis was used to determine amongst which samples the differences lay.

A one-way ANOVA was again selected to discriminate differences in the D-lactate data. The D-lactate assay however, yielded data only for the West coast animals and so the ANOVA performed compared D-lactate levels amongst animals belonging to different treatments, over time. Residuals were again tested for normality and homoscedasticity. The one-sample Kolmogorov-Smirnov test revealed that the data were not normally distributed

and hence an independent-samples Kruskal-Wallis test was used keeping a 5% significance level.

All proteomic data were analyzed using one-way ANOVAs. Differences were assessed amongst treatment groups within populations, i.e. comparing control, 16°C±2 and 16°C±4 animals within each biogeographic region over time. Differences were also detected across populations for a single treatment, also determined over time. Residual testing revealed that the carbonyl content data for the West coast animals was not normal distributed. An independent-samples Kruskal-Wallis test was used to determine if differences were present in these data, using a 5% significance level.

Lastly, differences at the transcriptomic level were assessed within and across groups from different biogeographic regions using one-way ANOVAs using time and treatment as factors. This was followed by assumptions testing using the one-sample Kolmogorov-Smirnov test for normality and the Levene's test for homoscedasticity. All data were found to not be normally distributed and thus independent-samples Kruskal-Wallis tests were used (with 5% significance levels). No statistical differences were detected and thus no post-hoc analyses were performed.

All statistical tests were performed on original data (i.e. prior to normalization) using SPSS® Statistics Version 21 (IBM®). Results figures were constructed using GraphPad Prism (v6.03).

3. RESULTS

3.1. Organismal Level Responses

Initial analyses of all the biological responses assessed revealed there to be no significant differences in the control variables within each biogeographic region when compared over time (Table 3.1.). The data presented below are thus normalized against their respective controls as these were treated as single mean values due to the lack of statistical variation over time.

Table 3.1: *P*-values for all biological responses measured, where *n* = 6 for all responses excluding D-lactate (*n* = 5) and carbonyl (*n* = 4) accumulation.

	Oxygen consumption	Ammonia excretion	O:N ratio	D-lactate accumulation	Carbonyl accumulation
West Coast	<i>P</i> = 0.116	<i>P</i> = 0.080	<i>P</i> = 0.115	<i>P</i> = 0.851	<i>P</i> = 0.755
East Coast	<i>P</i> = 0.531	<i>P</i> = 0.067	<i>P</i> = 0.530	---	<i>P</i> = 0.660

Note: D-lactate was not detected for East coast animals. *Hsp70* gene expression controls were all normalized to 1 using the $2^{-\Delta\Delta Ct}$ method and thus were excluded from the table.

Initial inspection of all the biological responses assessed supported the validity of the values obtained for the treatment groups as the majority of the control values fell within ranges observed in other studies. Vosloo and Vosloo (2010) reported oxygen consumption rates between 20 and 30 $\mu\text{mol kg}^{-1} \text{min}^{-1}$ for cold acclimated *H. midae* kept at 16°C which are rates slightly above those found in the present study (Table 3.2.). Ammonia excretion rates for abalone maintained at 16°C were found to vary between 4.5 and 7 $\mu\text{mol kg}^{-1} \text{min}^{-1}$ (Vosloo and Vosloo, 2010) which was observed for the East coast animals, while that of the West coast animals varied from 7.52 ± 0.52 to 10.89 ± 1.02 $\mu\text{mol kg}^{-1} \text{min}^{-1}$ over time (Table 3.2.). The range of O:N ratios seen in abalone from both biogeographic regions fell within that reported by Vosloo and Vosloo (2010) which was between 15 and 30 for abalone kept at 16°C. D-lactate accumulation in animals from the present study was lower than that recorded by Vosloo and Vosloo (2010) (0.02 to 0.07 mmol L^{-1}), while carbonyl accumulation was within the reported range of approximately 7.5 to 12.5 nmol carbonyl

mg protein⁻¹ (Vosloo *et al.*, 2013). Differences reported here may be due to individual variation or may be due to differences in acclimatory conditions.

Table 3.2: The mean and standard error values for the control groups of the biological responses assessed (excluding *hsp70* gene expression), with n = 6 excepting for D-lactate (n = 5) and carbonyl (n = 4) accumulation.

	West coast				East coast			
	Day 1	Day 3	Day 7	Day 14	Day 1	Day 3	Day 7	Day 14
Oxygen consumption (μmol kg ⁻¹ min ⁻¹)	17.78 ±0.76	20.45 ±1.92	19.61 ±0.92	16.67 ±1.01	16.99 ±1.25	14.83 ±1.39	14.89 ±0.71	14.73 ±1.01
Ammonia excretion (μmol kg ⁻¹ min ⁻¹)	7.52 ±0.53	8.02 ±1.90	9.78 ±0.37	10.89 ±1.02	4.84 ±1.32	7.77 ±0.67	5.86 ±0.44	5.25 ±0.46
O:N ratio	35.56 ±1.52	40.89 ±3.84	39.23 ±1.83	33.33 ±2.02	33.98 ±2.50	29.66 ±2.78	29.78 ±1.43	29.46 ±2.01
D-lactate accumulation (mmol L ⁻¹)	0.010 ±0.021	0.020 ±0.046	0.003 ±0.008	0.018 ±0.028	---	---	---	---
Carbonyl accumulation (nmol carbonyl mg protein ⁻¹)	9.99 ±0.99	7.71 ±0.32	7.54 ±0.94	7.41 ±0.95	12.87 ±2.44	11.28 ±2.05	11.95 ±1.79	11.05 ±1.77

Note: The *hsp70* gene expression control values all equalled 1 as a result of $2^{-\Delta\Delta Ct}$ calculation normalization thus warranting elimination from the above table. D-lactate was not detected for East coast animals.

3.1.1. Oxygen Consumption Rates

Treatment group animals from both the West and East coasts showed initial increases in oxygen consumption upon exposure to thermal stress (Figure 3.1.), when normalized against control animals. For the West animals (Figure 3.1. a.) this initial increase in oxygen consumption was found to not be statistically significant, while for the Eastern animals statistical significance ($P < 0.001$) was found only for the 16°C±4 group (Figure 3.1. b.). The peak in oxygen consumption for the 16°C±2 group of the Eastern animals, although

not being significantly different from the other treatments, was noted to only occur at day 3 of exposure.

The oxygen consumed by West animals (Figure 3.1. a.) then decreased to below control levels and was markedly lower for the $16^{\circ}\text{C}\pm 2$ group. This decline was greatest at day 3 and was statistically significant for both of the treatment groups ($P < 0.001$). Thereafter, the oxygen consumed by both of the West coast treatment groups began rising to surpass control levels after day 7 and resulted in rates that were significantly different from the control ($P = 0.004$ and $P = 0.002$ for the $16^{\circ}\text{C}\pm 2$ and $16^{\circ}\text{C}\pm 4$ groups respectively).

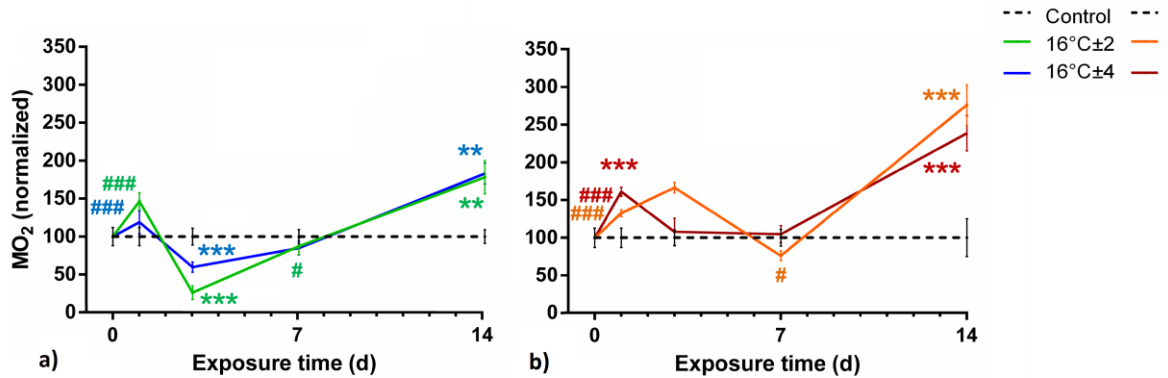


Figure 3.1: The oxygen consumption (MO_2) of exposed West (a) and East coast animals (b) normalized against that of the control animals for each respective region. Error bars denote standard error and significant differences are denoted by asterisks (*) where * indicates $P < 0.05$, ** indicates $P < 0.01$ and *** indicates $P < 0.001$ when comparing treatment groups to the control. Significant differences across regions are indicated by hash symbols (#) where # shows $P < 0.05$, ## shows $P < 0.01$ and ### shows $P < 0.001$. The color of the symbols corresponds to the treatment group as indicated by the key ($n = 6$ for the control and $n = 5$ for the treatment groups).

The oxygen consumed by the East coast animals also declined (relative to the control) after the initial spike (Figure 3.1. b.), as was noted for the West coast animals. The $16^{\circ}\text{C}\pm 4$ group showed this reduction in oxygen consumption rates after day 1 of exposure, while this decline was delayed in the $16^{\circ}\text{C}\pm 2$ group occurring only at day 3. The oxygen consumed by animals from both treatment groups then increased after day 7, as was seen with the West coast animals, and was at its highest by day 14 ($P < 0.001$ for both groups). The oxygen consumption rates by the end of the exposure were slightly higher for the

16°C±4 group of the West coast animals, while for the East coast animals this was true for the 16°C±2 group.

When comparing the oxygen consumption rates of the animals across biogeographic regions, similar responses were noted in animals belonging to the same treatment group. The oxygen consumption rates of all the control animals (West and East coast) displayed a negative trend over time which was not supported statistically. The baseline oxygen consumption rates for the East coast animals was found to be lower than that of the West coast animals (Table 3.2.), while the treatment animals showed increased oxygen consumption rates (relative to the control) over time, with the only statistical difference between the two populations being found at day 1 (Figure 3.1.). The mean oxygen consumption rates for the East coast animals were found to be almost double those of the West coast animals (27.78 ± 1.00 vs $14.23 \pm 1.12 \mu\text{mol kg}^{-1} \text{min}^{-1}$ respectively) when comparing the 16°C±2 groups ($P < 0.001$), and to be more than double (33.68 ± 1.33 vs $11.56 \pm 1.49 \mu\text{mol kg}^{-1} \text{min}^{-1}$ respectively) when comparing the 16°C±4 groups ($P < 0.001$).

3.1.2. Ammonia Excretion Rates

The rate at which ammonia was excreted by treatment animals from both regions remained low for the majority of exposures when compared to that of the control animals (Figure 3.2.). For the West coast animals (Figure 3.2. a.) an initial decrease in ammonia excretion was noted at day 1 for both treatment groups, but was statistically significant only for the 16°C±2 group. This group (16°C±2) was found to be significantly different from both the control group ($P = 0.001$, green asterisks on Figure 3.2. a.) and the 16°C±4 group ($P = 0.011$, black asterisk on Figure 3.2. a.).

This decrease was followed by some non-significant fluctuations with a significant decline in ammonia excretion rates being observed at day 7 ($P = 0.019$). This significance however, was valid only for the 16°C±2 group. Both treatment groups had significantly lower ammonia excretion rates by the end of exposure when compared to the control (blue and green asterisks respectively) and when compared to each other (black asterisks) with $P < 0.001$ in all cases.

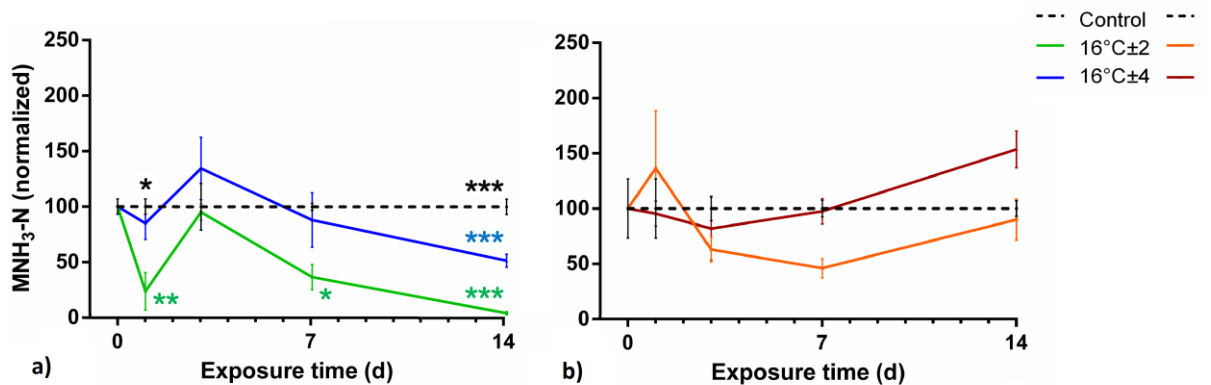


Figure 3.2: The ammonia excretion ($\text{MNH}_3\text{-N}$) of the exposed West (a) and East coast (b) animals normalized against that of the control group for each region. Asterisks (*) and hash symbols (#) denote the degree of significant differences ($P < 0.05$, $P < 0.01$ or $P < 0.001$) when comparing treatment groups to the control. Asterisks represent within population significances while hash symbols show across population differences. The treatment is indicated by the color of symbols as show by the key. Error bars indicate standard error ($n = 6$ for the controls while $n = 3$ for the treatment groups).

Despite the lack of significant variation in the ammonia excretion data for either of the East coast treatment groups when assessed over time, it was noted that the ammonia excreted by the $16^\circ\text{C}\pm 2$ group was below that seen for the $16^\circ\text{C}\pm 4$ group, from day 3 onward. This trend was also observed with the West coast treatment groups. Interestingly, a higher degree of variability in response was displayed (see standard error bars), especially by the $16^\circ\text{C}\pm 2$ treatment group of the East coast animals at day 1. The mean ammonia excretion rate for this group ($16^\circ\text{C}\pm 2$) was however, found to be significantly lower than the control mean ($P = 0.024$) when time was disregarded as a factor.

Statistical differences were also not detected when comparing the ammonia excretion rates of treatment animals across biogeographic regions. The start and end ammonia excretion rates for the West coast control animals were found to be almost two times ($P = 0.015$ for day 1) and three times greater ($P < 0.001$ for day 14) than that of the East coast animals at the same time points, despite East coast animals appearing to have higher ammonia excretion rates. This however, was as a result of lower baseline (i.e. control) ammonia excretion rates for the East coast animals.

3.1.3. Oxygen: Nitrogen Ratios

The O:N ratios for animals from both regions (Figure 3.3.) showed trends which were similar to those seen for ammonia excretion in that an increase in O:N ratios was observed at the beginning of exposures which resulted in lowered levels for the West coast animals (Figure 3.3. a.) towards the end of exposures, and elevated levels for the East coast animals relative to the control (Figure 3.3. b.).

Both of the treatment groups from the West coast experienced a spike in the O:N ratio at day 1 that was significant only for the $16^{\circ}\text{C}\pm 2$ group with $P = 0.023$ when compared to the control and $P = 0.026$ when compared to the $16^{\circ}\text{C}\pm 4$ group (Figure 3.3. a.). The O:N ratio then decreased for both treatment groups with that of the $16^{\circ}\text{C}\pm 4$ group remaining close to control levels. By the end of exposure, the O:N ratios of both treatment groups were still below control levels with the $16^{\circ}\text{C}\pm 2$ group being statistically lower than both the control ($P = 0.002$) and the $16^{\circ}\text{C}\pm 4$ group ($P = 0.006$).

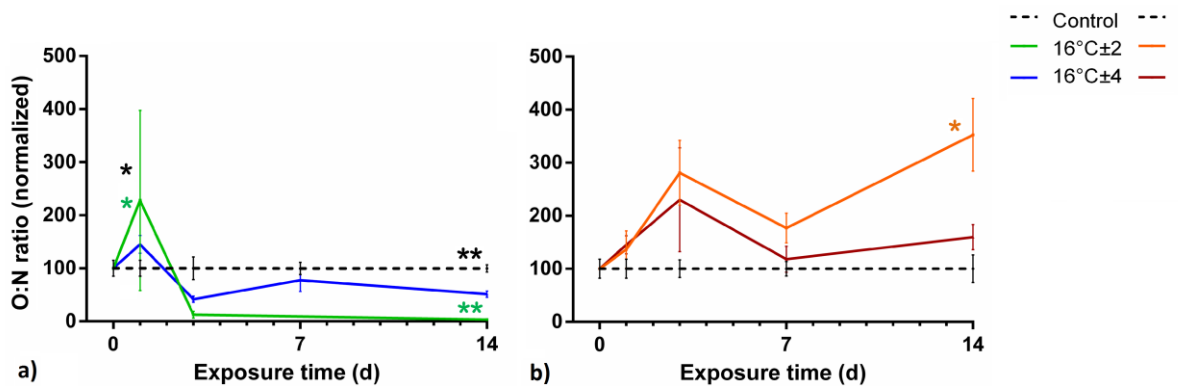


Figure 3.3: Oxygen: nitrogen (O:N) ratio of West (a) and East (b) coast animals using control values for normalization of treatments. Significant differences ($P < 0.05$, $P < 0.01$ or $P < 0.001$) are denoted by asterisks (*) or hash symbols (#) where colored symbols (see key) indicated differences between treatments and the control and black symbols show differences between treatment groups themselves. Standard error denoted by error bars ($n = 6$ for the controls and $n = 3$ for the treatments).

The East coast animals also showed an initial spike in O:N ratio, although occurring later (at day 3) and being non-significant, when compared to the West coast animals (Figure 3.3. b). The lack of significance may be attributed to the great variation in O:N ratios at this

point. The $16^{\circ}\text{C}\pm 2$ group displayed O:N ratios greater than the $16^{\circ}\text{C}\pm 4$ group for the duration of exposures, but this was only statistically significant when compared to the control group at day 14 of exposure ($P = 0.035$).

No significant differences were detected when comparing treatment groups across biogeographic region. It was however, noted that the O:N ratio, like the ammonia excretion rates, appeared to be higher for the East coast animals. This was once again due to the normalization of data against the controls, with both West coast and East coast treatment animals showing O:N ratios which were lower than 10 by day 14.

3.2. Biochemical Level Responses

3.2.1. D-lactate Accumulation

Low amounts of D-lactate were detected for animals from the West coast, with the $16^{\circ}\text{C}\pm 2$ animals producing levels of D-lactate which appeared lower than those of the control animals for the entire duration of the exposure (Figure 3.4.). The D-lactate produced by the $16^{\circ}\text{C}\pm 4$ group of the West coast animals appeared slightly greater than that of both the control and $16^{\circ}\text{C}\pm 2$ groups, this showing more prominence at day 1 and day 7 of exposure. These increasing trends noted at days 1 and 7, although not statistically significant, were accompanied by high degrees of variation in the amounts of D-lactate accumulated by animals most notably those from the $16^{\circ}\text{C}\pm 4$ group.

D-lactate, though still being detected in the assay standard provided by the Megazyme kit, was not detected in any of the samples obtained from the East coast animals.

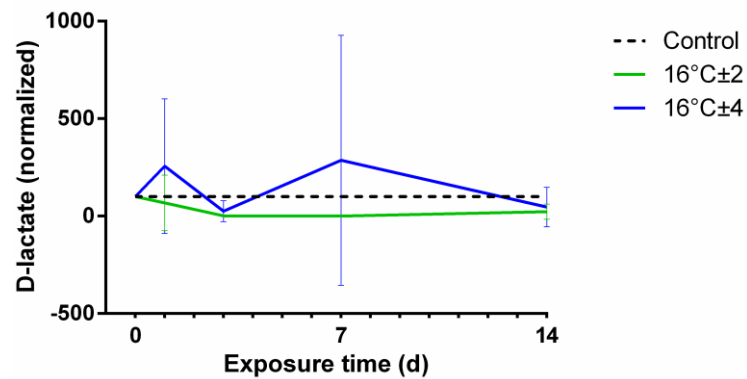


Figure 3.4: The D-lactate produced by the West coast animals normalized against that of the control animals. Error bars symbolize standard error ($n = 5$ for both treatments and control).

3.3. Proteomic Level Responses

3.3.1. Stress Protein (Hsp70) Response

Dot blots were employed to quantify the proteomic response (using Hsp70 antibody) of thermally stressed animals. Hsp70 proteins however, were unable to be quantified using the blots due to an excessive background signal (Figure 3.5.; for detailed troubleshooting procedure see Appendix A.2.4.). The blots did however, confirm the presence of Hsp70 in the samples (light dots produced on all membranes) but in unknown relative quantities.

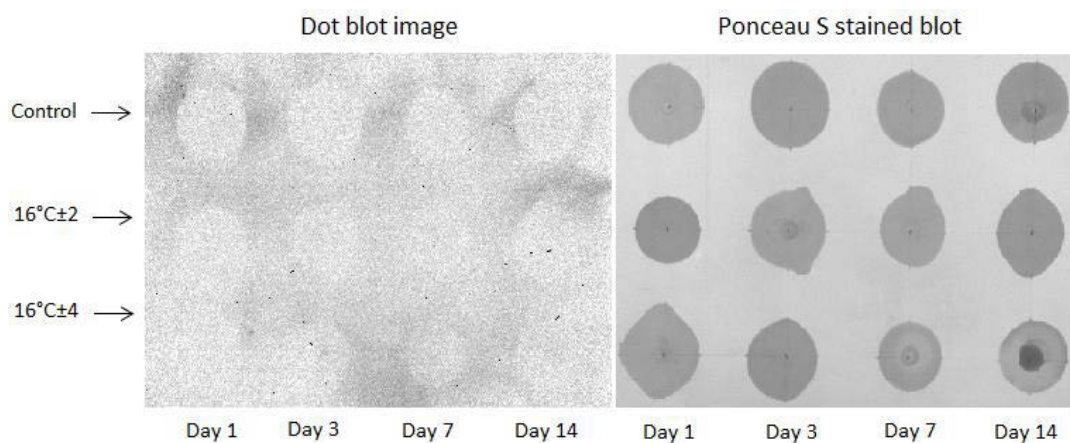


Figure 3.5: Representation of a dot blot indicating high background signal, shown with accompanying Ponceau S stained blot indicating the presence of protein. Illustration shows dot blot of samples taken from West coast reared abalone.

3.3.2. Oxidized Protein Responses

Similar expression profiles were displayed by both of the treatment groups from the West coast (Figure 3.6.). Both West coast treatment groups showed non-significant elevations in carbonyl content at the start of exposures, at day 1 and 3 for the 16°C±2 and 16°C±4 groups respectively. Another non-significant increase was observed but only for the 16°C±2 group at the end of exposures. The 16°C±4 group had carbonyl levels below those of the control from day 7 onwards, while both East coast treatment groups had below control levels of carbonyls for the duration of exposure.

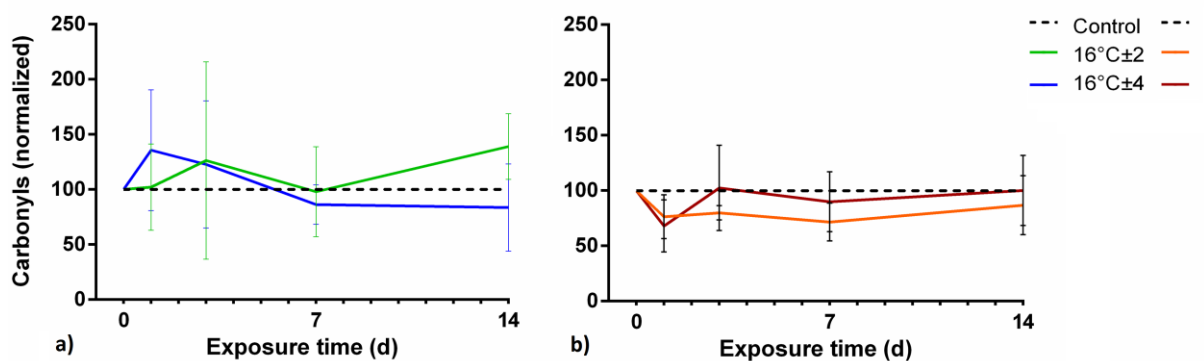


Figure 3.6: Amounts of carbonylated protein detected for West coast (a) and East coast (b) animals, normalized against their respective control values. Error bars indicate standard error (n = 4 for the treatments and controls).

Similar patterns of carbonylated protein accumulation were also detected for the treatment groups of the East coast animals, but with the 16°C±4 group showing carbonyl levels which appeared slightly higher than those of the 16°C±2 group (Figure 3.6. b.). A non-significant decrease in carbonyl content was however, noted for both treatment groups at day 1. The amounts of carbonylated proteins produced by both treatment groups during the latter half of exposure showed apparent slight increases, approximating control levels with the carbonyl levels of the 16°C±4 group remaining above those of the 16°C±2 group.

Neither of the treatment groups of the animals from the West or East coasts showed any significant variation when compared to each other, again as a result of the high variation at all the time points assessed. It was however, observed that the baseline carbonyl content for

the East coast animals was higher than that of the West coast animals (10.24 ± 0.94 and 8.16 ± 0.47 carbonyls per μg of protein respectively), albeit non-significantly.

3.4. Transcriptomic Level Responses

3.4.1. RNA Integrity Validation

The integrity of all RNA samples used for the construction of cDNA for qPCR purposes was assessed by agarose gel electrophoresis (refer to section 2.9.1. of Materials and Methods) and found to be intact (Figure 3.7.).

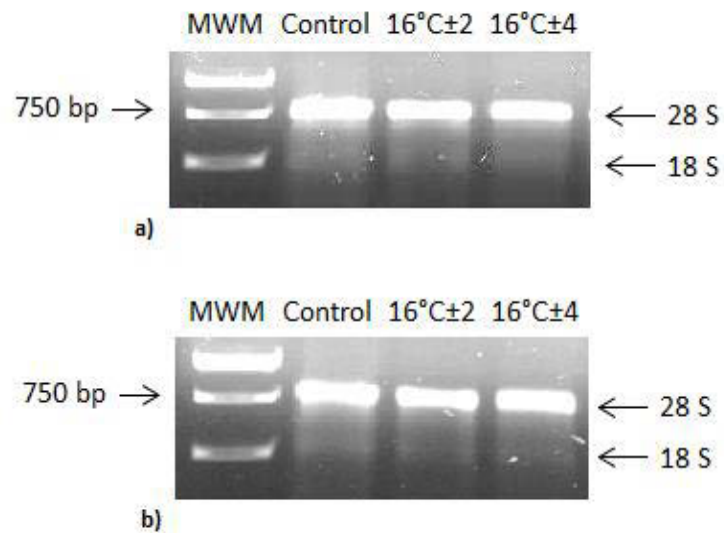


Figure 3.7: Validation of the presence of the 28 S and 18 S rRNA subunits of intact RNA. RNA shown above extracted from the first biological repeat of the West coast (a) and East coast (b) samples. (MWM indicates molecular weight marker).

3.4.2. Relative *Hsp70* Expression

West coast animals showed non-significant elevations in the *hsp70* expression of the 16°C±4 group at day 1 and day 7 (Figure 3.8. a.), which were once again accompanied by high amounts of variation amongst individuals assessed. The 16°C±2 group on the other hand maintained near control levels of *hsp70* expression with a moderate increase, occurring from day 7 of exposure onward, resulting in expression levels which seemed greater than those of both the control and 16°C±4 groups by day 14.

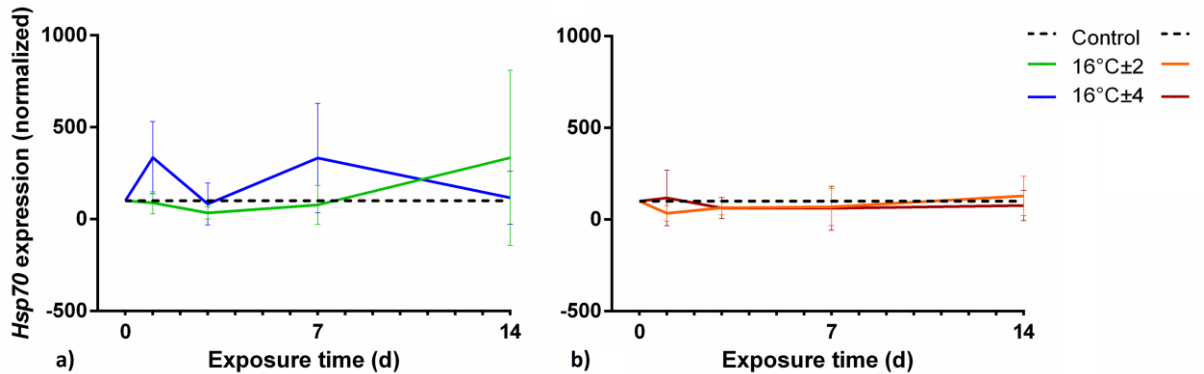


Figure 3.8: The *hsp70* levels (expressed relative to *coxIII*) of West coast (a) and East coast (b) animals. The relative expression of the treatment groups (16°C±2 and 16°C±4) is normalized to the control levels over the two week exposure and error bars denote standard error (n = 3).

Both East coast treatment groups displayed *hsp70* expression levels below those of the control for the majority of the exposure period with no significant differences being detected between any of the groups (Figure 3.8. b.). The degree of variation displayed by the individuals of both East coast treatment groups was noted to be lower than that seen for the West coast animals at every time point analyzed.

Differences across any of the treatment or control groups of the animals from the two biogeographic regions were again found to not be statistically significant, it was however, noted that the normalized *hsp70* expression appeared marginally higher for West coast animals especially for the 16°C±4 group (Figure 3.8. a.).

4. DISCUSSION

Numerous abiotic factors, such as salinity, pH, aeration, sunlight and humidity, have been shown to influence the distribution of species in the natural environment (Osovitz and Hofmann, 2005). Of these factors, the one which has been found to have the greatest effect in setting species boundaries is temperature (Hofmann, 2005). Temperature effects are of greater importance for sessile, ectothermic marine organisms (Hofmann, 2005) as they are unable to migrate during unfavourable conditions, but rather have to find methods of coping to the new conditions.

The effect of temperature on species distribution has been receiving heightened interest because of concerns regarding global climate change (Hofmann, 2005). Global climate change has been attributed to being the cause of several of the alterations in species distributions that have already been noted. Studying the current effects of temperature on organisms may provide an understanding into the mechanisms which determine the thermal tolerances of organisms able to survive in ever-changing environments. Gaining insight into current coping mechanisms may provide a method of predicting the responses that organisms may have to future thermal stress (Osovitz and Hofmann, 2005; Tomanek and Zuzow, 2010).

4.1. Metabolic Modification in Response to Thermal Stress

4.1.1. Organismal Level Adjustments

At the organismal level the stress response of the West coast reared animals was initiated earlier and to a smaller degree (relative to the control) when compared to that of animals reared on the East coast which had a prolonged acclimatory response (see Figure 3.1. and Figure 3.3.). These animals (Eastern) showed the greatest initial increases in oxygen consumption and O:N ratio on day 3 of exposure and not day 1 as was the case for the Western reared animals.

The elevated oxygen consumption rates noted at the end of exposures for abalone from both biogeographic regions (Figure 3.1. a. and b.) highlight the need for the organisms to obtain greater amounts of oxygen to maintain metabolism as is common in response to functional hypoxia (i.e. oxygen limitation due to the inability of the organism to supply the demand for it) (Lee and Lee, 2011). It remains unknown however, if abalone are able to maintain

metabolism for prolonged periods at these newly increased oxygen consumption rates. It is possible that abalone may be able to rearrange their metabolic processes after prolonged exposure, as was observed in abalone exposed to high (22°C), constant temperatures for one month (Vosloo and Vosloo, 2010).

The prolonged reliance on elevated rates of oxygen consumption does however, have negative implications due to the association with the increased activity of the electron transport chain (ETC). An accelerated ETC results in electron leakage, increased ROS production and DNA damage (by ROS) and protein damage (through carbonylation) (Vosloo *et al.*, 2012). Combating ROS is an ongoing task as the internal environment must remain reduced, despite the oxidizing influence of the external environment (McDonagh *et al.*, 2005), and so any perturbations may result in the mismatch of ROS producing and ROS eliminating processes (Scandalios, 2005).

It was however, noted that animals from both biogeographic regions experienced a period of decreased oxygen consumption (Figure 3.1.). For the West coast animals this occurred from day 1 to day 3 of exposure while this response was more pronounced for the East coast animals and occurred from day 1 to day 7. A reduction in oxygen consumption during stress is consistent with the reduction of mitochondrial respiration in an attempt to reduce the amounts of ROS being produced (Vosloo *et al.*, 2013). Low levels of ATP, which result when mitochondrial respiration is reduced, then act to trigger the transcription of mitochondria so that respiration can be restored (Vosloo *et al.*, 2013). Increased levels of mitochondrial transcription thus increase respiration rates as reflected by the increase in the oxygen consumption noted after day 7 for both West coast and East coast animals (Vosloo *et al.*, 2013).

The ammonia excretion rates for animals from both regions appeared to be low when compared to the control for that respective group (Figure 3.2.) it was however, noted that the overall system free ammonia nitrogen (FAN) levels for animals reared on the West coast was more than three times greater than that for the animals reared on the East coast (Table 2.1). FAN, due to its readiness to diffuse across membranes, is the more toxic form of ammonia (Lyon, 1995). This metabolite is correlated with reductions in the growth rates of commercially reared abalone and is detrimental to overall animal health (Reddy-Lopata *et al.*, 2006; Naylor *et al.*, 2011).

A mechanism proposed to be responsible for poor animal health is the inability of animals to obtain adequate amounts of oxygen as a result of the physiological changes incurred to the gills (Lyon, 1995). FAN values as low as $4 \mu\text{g L}^{-1}$ have been reported as lowering growth rates, provided that these coincide with conditions of low pH (Naylor *et al.*, 2011). Higher rates of ammonia excretion are not only toxic to the health of organisms but are also indicative of protein catabolism (Naylor *et al.*, 2011). This finding was confirmed by the low values obtained for the O:N ratios, specifically for the West coast animals (Figure 3.3.).

The O:N ratios of animals from both biogeographic regions were low towards the end of the exposure, with animals from the West coast showing O:N ratios lower than those of the control groups which was not observed for the East coast animals (Figure 3.3.). Low O:N ratios are indicative of a switch from carbohydrate and/ or lipid based metabolism to one fuelled by protein (Vosloo *et al.*, 2012). Protein based metabolism cannot be relied on for sustained periods though as animals relying on proteins may also begin breaking down their own structural proteins to fuel metabolism resulting in tissue wasting (Vosloo *et al.*, 2012). Protein based metabolism is sufficient only in maintaining basal metabolism meaning that the survival of the animal is promoted but not growth (Vosloo *et al.*, 2013). Abalone exposed to fluctuating temperatures are thus likely to be in poor health which ultimately impacts on the abalone industry unfavorably. East coast animals, although appearing to have O:N ratios which may be considered in the healthy range (higher values in comparison to the controls), also had O:N ratios below 10 for the latter half of exposures and most notably for the $16^{\circ}\text{C}\pm 4$ group.

The organismal level processes of *H. midae* were elevated in response to fluctuating temperatures indicating the perception of stress. All responses displayed a transitory period during the first week of exposure which by the end of exposures had resulted in metabolic readjustments enabling the physiological processes to be maintained at heightened rates. Of all the physiological responses assessed the only one found to show any statistical differences across biogeographic regions was oxygen consumption rate (Figure 3.1.). This highlights the importance of the role of oxygen in determining thermal tolerance (Pörtner and Farrell, 2008).

4.1.2. Biochemical Level Adjustments

Low amounts of D-lactate were detected for the West coast reared animals with none being detected for their Eastern counterparts. The amounts of D-lactate found appeared greatest for the 16°C±4 group although no statistical differences were found (Figure 3.4.). These findings suggest that further analysis is required by, for example, increasing the sample size, especially for West coast reared abalone as these animals displayed greater variability in individual responses. The detection of D-lactate from the West coast samples alone suggests that only this group of animals underwent anaerobic metabolism due to the presence of the end-product of the D-lactate pathway (Lee and Lee, 2011). This pathway is initiated in order to maintain or increase metabolic activity (Livingstone, 1991) and may be responsible for the elevated rates of oxygen consumption observed for the West coast reared animals during the last week of exposures (Figure 3.1.). The D-lactate pathway is useful in maintaining optimal levels of metabolism as it produces high rates of energy (Livingstone, 1991). The drawback however, is the wastefulness of this pathway as greater amounts of substrate are required for energy production (Livingstone, 1991). The substrate utilized by this pathway is carbohydrate which does not occur in abundant amounts in *H. midae* (Livingstone, 1991), thus bringing into question the sustainability of this method of metabolism in the long-term because of the diminished growth rates as a result of excessive substrate consumption (Livingstone, 1991).

The activation of the D-lactate pathway only in abalone from the West coast was consistent with the higher amounts of FAN recorded for this group (Table 2.1). The inability of the gills to obtain sufficient oxygen, which may occur if oxygen is out-competed by ammonia, triggers the switch to anaerobic metabolism (Lyon, 1995; O'Omolo *et al.*, 2003). This thus suggests that West coast reared abalone were more stressed by the thermal fluctuations and thus needed a mechanism to supplement metabolism (Lee and Lee, 2011).

Although the trends seen in the accumulation of D-lactate for the West coast animals were random (i.e. not statistically significant), it is interesting to note that periods of seeming increases in D-lactate coincided with periods of increased oxygen consumption (Figure 3.1.). If this were to be confirmed statistically for the West coast animals it would be validated by the fact that the D-lactate pathway is utilized for the maintenance of metabolism as previously mentioned (Livingstone, 1991). East coast abalone also experienced periods of decreased oxygen consumption followed by increased rates which were likely supported by a

secondary metabolic pathway. It may be possible that the East coast animals were utilizing an alternative anaerobic pathway (viz. the opine pathway) as this would explain the reason for the lack of D-lactate detection for this group.

The opine pathway is favored in lower, less active animals because the end-products made are smaller than D-lactate and are more efficiently eliminated (Lee and Lee, 2011). The substrate utilized by the opine pathway is amino acids, which occur more abundantly in marine invertebrates due to the alternate role they play in osmoregulation (Lee and Lee, 2011). The possible use of an amino acid utilizing anaerobic pathway is supported by the fact that such pathways decrease proton leakage and increase the oxygen efficiency associated with the catabolism of protein (Vosloo *et al.*, 2013).

4.1.3. Proteomic Level Adjustments

Hsp70 was unable to be quantified but it is conceivable, based on protein detection by Ponceau S staining and the results obtained from previous results (Appendix A.2.4.), that the inverted dots produced on membranes were a result of the presence of Hsp70 (Figure 3.5.). Previous work (Honors project, 2011), which indicated the presence of Hsp70 by Western blot (Figure A.2.4.1.), is comparable to the current work as animals were exposed to fluctuating temperatures with the only differences being the amount of time that animals were exposed for. Whether the protein dots present on blots represent the induction of the thermal stress response or not remains unclear as Hsp70 is not only expressed during stressful conditions, but also functions as a house-keeping chaperone during favorable conditions (Sørensen *et al.*, 2003). The presence of Hsp70 would indicate active repair processes only and not an indication of the level of protein damage incurred if any (Hofmann and Somero, 1995). Identifying protein modifications via carbonylation, on the other hand, is a method for assessing permanent protein damage (Nyström, 2005).

Despite the lack of significant differences in the carbonyls detected between the control and treatment groups for the West and East coast animals over time, carbonyls were still found to be present in the samples taken from both biogeographic regions (Figure 3.6.). Whether carbonyl levels do in fact increase towards the end of exposures as was suggested by the trends seen especially from the West coast animals requires further analysis, past the two week mark. Extensive protein carbonylation results in the decrease in the catalytic activities of the targeted proteins (due to conformational changes) and may lead to the formation of

high molecular weight protein aggregates (Nyström, 2005). These aggregates are cytotoxic due to their inability to be degraded (Nyström, 2005), excessive carbonylation would thus be detrimental to abalone health.

Animals reared on the East coast appeared to maintain low carbonyl levels for the duration of the exposure, when compared to their respective control group (Figure 3.6. b.). It was however, noted that the East coast reared animals had higher baseline carbonyl (i.e. control) values when compared to the West coast animals (Table 3.2.). High carbonyl content has previously been found in control samples and was related to the fact that the tissue from which the samples were taken was partially oxidizing (McDonagh *et al.*, 2005). This however, was not the case for the East coast animals as the tissue samples for this group were the same as those sampled for the West coast group. High starting carbonyl levels may thus be an indication of on-going damage that may be experienced by the East coast reared animals which would suggest that the seemingly low physiological responses observed represent the inability of these animals to initiate protective responses sufficient enough to prevent molecular damage.

4.1.4. Transcriptomic Level Adjustments

Although the relative *hsp70* transcription levels appeared to be greater for the West coast reared animals (most notably the 16°C±4 group) when compared to the East coast animals, none of these differences were statistically significant (Figure 3.8.). Significant increases in *hsp70* production, which may arise in the West coast reared animals after the two week exposure (see 16°C±2 group), would be indicators of perturbations to the protein pool which require the stabilizing capabilities of Hsp70 (Buckley *et al.*, 2001). Thermal stress upregulates the transcription of *hsp70* and it is interesting to note that significant increases in this response were not detected for either of the biogeographic populations assessed (Figure 3.8. b.).

In an attempt to understand organismal function, assessing and understanding the processes which occur at the lowest level of organization (i.e. transcriptional level) assist in revealing where potential limitations may lie (Vosloo *et al.*, 2013). In light of this statement it seems possible that the adaptive limitations that may exist, especially in the East coast abalone, may lay in their apparent inability to initiate a strong enough transcriptional response of *hsp70* to repair any damage which may have resulted from the thermal fluctuations (Figure

3.8.). Because both West and East coast animals were allowed to acclimate under the same conditions it is unlikely that differences in levels of *hsp70* transcription, that may become more pronounced after two weeks of exposure, would be due to the recent thermal histories of the organisms as this would mean different *hsp70* induction temperatures (Dahlhoff, 2004).

The upregulation of *hsp70* transcription may be repressed in East coast animals, a mechanism which occurs as the result of the preferential carbonylation of Hsp70 (Nyström, 2005). This Hsp70 carbonylation is due to increases in the accumulation of protein aggregates, proteins which themselves have been carbonylated and thus cannot be tagged for degradation by Hsp's (Vosloo *et al.*, 2013). The lack of a damaged protein stimulus thus ensures that Hsp70 levels remain low.

Because the responses at the transcriptomic level were non-significant and also because responses at this level can't always be correlated with those at higher levels of organization (Podrabsky and Somero, 2004), this study may have benefitted from the assessment of the antioxidant capacity of the abalone. Analyzing antioxidant capacity, for example by using the ferric reducing ability of plasma (FRAP) assay, would have made clearer if the damage preventing ability of the animals had been impacted upon and if a need for protein repair mechanisms had arisen (Vosloo *et al.*, 2013).

4.2. Overall Aerobic Performance of West Coast vs East Coast Animals

Animals from both the West and East coasts demonstrated significant elevations in oxygen consumption by the end of the two week exposure (Figure 3.1.). This indicates that both populations of abalone had lost aerobic performance as a result of exposure to fluctuating temperature (i.e. T_p 's were exceeded) (Pörtner and Farrell, 2008).

Not only were T_p 's surpassed, but T_c 's may have also been exceeded. This was suggested by the transient switches to anaerobic metabolism as displayed by the West coast reared abalone (Figure 3.4.). The lack of D-lactate detection for the East coast abalone may be due to the utilization of an opine pathway, which would mean that the aerobic performance and thus the thermal resistance of both populations of animals may have been further impacted on due to the onset of anaerobiosis (Pörtner and Knust, 2007; Pörtner and Farrell, 2008).

Beyond T_p , denaturation temperatures (T_d) ensue where Hsp70 is initiated for the repair of proteins or alternatively, excessive protein damage occurs which may manifest as carbonylation (Nyström, 2005). The transcription of *hsp70* appeared slightly elevated in West coast animals which, if after further investigation, was to be significant would indicate the initiation of the heat shock pathway in response to thermal fluctuations (Figure 3.8. a.), or a retained ability to do so. The lack of difference in the *hsp70* levels shown between the treatment and control groups of the East coast animals (Figure 3.8. b.), on the other hand, may illustrate that East coast animals may not be stressed by thermal fluctuations at the transcriptomic level and therefore had no need to increase *hsp70* gene transcription.

Alternatively, low levels of *hsp70* may be an indication of the impediment of the ability to initiate the repair response which would partly explain the elevated carbonyl content observed for the control animals of this group (Table 3.2.). This is supported by the fact that carbonylated proteins cannot be targeted by Hsp70 and thus the *hsp70* response would not be initiated meaning that transcript levels would remain low (Vosloo *et al.*, 2013). Another possible explanation for the observation of low *hsp70* expression levels would be the utilization of alternative Hsp's. Large Hsp's were expressed in *A. limnaeus* when exposed to constant temperature, while fluctuating temperatures activated the expression of small Hsp's (Podrabsky and Somero, 2004). Small Hsp's function to stabilize denaturing proteins before large Hsp's are recruited to perform the repair processes (Garrido *et al.*, 2001), and if these small Hsp's were indeed used to cope with temperature fluctuations it would thus explain the lack of Hsp70 detection at the proteomic level.

If abalone from both West and East coasts were to show significant signs of having reached T_d 's then this would be of great concern, firstly because the temperatures that animals were exposed to were within the range regularly experienced by abalone on farms (Figure 1.3.) and were temperatures at which the performance of juvenile abalone is said to be optimal (Sales and Britz, 2001). The exception however, would be the fluctuating nature of the temperatures in the present case. Secondly, the reaching of the T_d 's would be an indicator of further limitations to aerobic performance and as a result a limitation in thermal tolerance (Pörtner and Farrell, 2008). The animals functioning at fluctuating temperatures would therefore be performing poorly with growth being affected under these conditions and would so be just maintaining metabolism for survival (Pörtner and Farrell, 2008; Vosloo *et al.*,

2013). This is supported by the observation of decreased production which is associated with times of increased temperature variability (M. Naylor² pers. comm., 2013).

These results may have further implications for the East coast reared abalone as this group may potentially experience delays in the initiation of physiological responses; may be unable to efficiently upregulate *hsp70* transcription and may have already accumulated carbonylated proteins from previous thermal stress events. It may however, be argued that the trends observed in the biological responses (with the exception of organismal level measures) of both West coast and East coast reared abalone may be of no importance due to a lack of statistical significance, despite what is known of the regulation of the thermal stress response. It is therefore imperative that certain aspects of this study are further confirmed in subsequent studies.

4.3. Conclusion and Future Considerations

The temperatures used in the present study occur within the range of temperatures that abalone would regularly encounter on farms. The stress responses observed are thus as a result of the fluctuations in temperature, with smaller temperature fluctuations producing moderate or delayed stress responses. Responses to greater temperature fluctuations produced greater stress responses in the West coast animals while the responses in East coast animals may potentially show the beginnings of limitations in adaptation. Animals from both regions were able to maintain metabolism such that survival was ensured but growth may have been impacted on due to a reliance on protein-fueled metabolism. The present study would thus benefit from incorporating an estimation of growth rates, which would be measured at the sampling times during the two week exposure.

To get a better understanding of how physiological responses are altered prior to limitations in adaptation more research should be invested into moderate temperature fluctuations ($16^{\circ}\text{C}\pm 2$) over the long term (Vosloo *et al.*, 2013). Broadening the range of biomarkers used at the various levels of organization may also assist in shedding light into the events leading up to adaptive limitation. For example, assessing the end-products of opine metabolism may be one way in which further insight can be gained into the maintenance of metabolism in East coast reared animals as they too experienced increases in metabolism that did not

² Mr M. Naylor, HIK Abalone Farm (Pty) Ltd., Church Street Extension, Hermanus, 7200, South Africa

appear to have been supported by D-lactate metabolism. Although D-lactate accumulation increases in most tissue types in response to functional anoxia, the most intense effect of functional anoxia is displayed by tauropine dehydrogenase (TDH) which in a study by O'Omolo *et al.* (2003) exhibited a five-fold increase when *H. midae* was subjected to exercise for a short period. It is thus possible that East coast animals may have utilized opines, which were not detected as a result of the exclusive use of a D-lactate assay.

Investing research into responses geared towards protection (i.e. antioxidants) would also be beneficial especially in cases such as this where the results of the repair response (i.e. heat shock proteins) were unknown. Assessing the antioxidant capacity of the animals may have demonstrated limitations, if any, in the molecular protection response (Pörtner, 2002), and given a reference point as to when repair response should be at work. Limitations to the protective response are also indicative of limitations in aerobic scope (Pörtner, 2008).

Alternatively a more sensitive and quantitative method of assessing Hsp70 could be employed, for example in the form of ELISAs (Lewis *et al.*, 1999), to determine the level of protein expression as a result of the heat shock response. Time could also be invested into the analysis of small Hsp's such as Hsp20 which are upregulated during temperature fluctuations but are expressed in the short-term (Podrabsky and Somero, 2004).

Monitoring the downstream effects of temperature fluctuations on the whole organism, in terms of growth or tissue quality, would also be beneficial to the abalone aquaculture industry. These data would give an indication of how the abalone would be affected (at the whole organism level) by thermal stress which is known to favor shell growth over that of tissue (Vosloo *et al.*, 2013).

The exposure of abalone to temperature fluctuations for a period of two weeks appears to elicit a stress response which requires metabolic readjustment to elevated levels of functioning (Figure 3.1.) and leads to a reliance on protein metabolism (Figure 3.3.). How the animals will cope with the fluctuations following a two week period is unknown but it is probable that animals from both populations are at risk of having their overall health impacted on and their biogeographic ranges altered as a result of the inability to cope with changing environmental temperatures. The data revealed that animals from both biogeographic regions responded similarly to thermal fluctuations (with respect to alterations to metabolic rate) and thus both populations of abalone would require more rigorous

management during thermally unpredictable periods to ensure no unnecessary losses in production.

The aquaculture industry would thus benefit from taking steps to support optimal abalone metabolism, during times when fluctuating temperatures are expected to persist for periods longer than two weeks. Such measures could consist of maintaining good water quality, optimizing stocking density and minimizing handling stress during routine tank cleaning (Lyon, 1995). More stringent control of these measures would be required during times of expected increases in temperature variability (i.e. during summers) (Figure 1.3.). Such changes however, would be difficult to enforce as the restructuring of farm operations whenever conditions become unfavorable require managing on a large scale.

On the other hand, aquaculture managers could invest into the supplementation of abalone feeds with amino acids such as L-proline (Vosloo *et al.*, 2013). L-proline has been found to afford thermal protection during high temperatures by protecting cells from oxy-radicals and through the stabilization of Hsp's (Vosloo *et al.*, 2013). Investment into feed supplementation need only occur during times when temperature fluctuations are anticipated and would be a more practical management alternative as only one step in the abalone maintenance process (i.e. feeding) would require alteration.

5. REFERENCE LIST

- Anestis, A., Lazou, A., Pörtner, H. O. and Michaelidis, B. (2007). "Behavioral, metabolic, and molecular stress responses of marine bivalve *Mytilus galloprovincialis* during long-term acclimation at increasing ambient temperature." *American Journal of Physiology - Regulatory, Integrative and Comparative Physiology*, **293**(2): R911-R921.
- Barry, J. P., Baxter, C. H., Sagarin, R. D. and Gilman, S. E. (1995). "Climate-related, long-term faunal changes in a California rocky intertidal community." *Science*, **267**(5198): 672-675.
- Branch, G., Branch, M. and Bannister, A. (1981). *The Living Shores of Southern Africa*. Cornell University, Struik: 272.
- Buckley, B. A., Owen, M.-E. and Hofmann, G. E. (2001). "Adjusting the thermostat: the threshold induction temperature for the heat-shock response in intertidal mussels (genus *Mytilus*) changes as a function of thermal history." *Journal of Experimental Biology*, **204**(20): 3571-3579.
- Bustin, S. (2000). "Absolute quantification of mRNA using real-time reverse transcription polymerase chain reaction assays." *Journal of Molecular Endocrinology*, **25**(2): 169-193.
- Bustin, S. A., Benes, V., Garson, J. A., Hellemans, J., Huggett, J., Kubista, M., Mueller, R., Nolan, T., Pfaffl, M. W., Shipley, G. L., Vandesompele, J. and Wittwer, C. T. (2009). "The MIQE guidelines: minimum information for publication of quantitative real-time PCR experiments." *Clinical Chemistry*, **55**(4): 611-622.
- Cook, P. A. and Gordon, R. H. (2010). "World abalone supply, markets, and pricing." *Journal of Shellfish Research*, **29**(3): 569-571.
- Dahlhoff, E. P. (2004). "Biochemical indicators of stress and metabolism: applications for marine ecological studies." *Annual Review of Physiology*, **66**(1): 183-207.
- Drew, B., Miller, D., Toop, T. and Hanna, P. (2001). "Identification of expressed Hsp's in blacklip abalone (*Haliotis rubra* Leach) during heat and salinity stresses." *Journal of Shellfish Research*, **20**: 695-703.
- Gäde, G. (1988). "Energy metabolism during anoxia and recovery in shell adductor and foot muscle of the gastropod mollusc *Haliotis lamellosa*: formation of the novel anaerobic end product tauropine." *The Biological Bulletin*, **175**(1): 122-131.
- Garrido, C., Gurbuxani, S., Ravagnan, L. and Kroemer, G. (2001). "Heat shock proteins: endogenous modulators of apoptotic cell death." *Biochemical and Biophysical Research Communications*, **286**(3): 433-442.
- Harley, C. D. G., Randall Hughes, A., Hultgren, K. M., Miner, B. G., Sorte, C. J. B., Thornber, C. S., Rodriguez, L. F., Tomanek, L. and Williams, S. L. (2006). "The impacts of climate change in coastal marine systems." *Ecology Letters*, **9**(2): 228-241.

- Hofmann, G. and Somero, G. (1995). "Evidence for protein damage at environmental temperatures: seasonal changes in levels of ubiquitin conjugates and hsp70 in the intertidal mussel *Mytilus trossulus*." *Journal of Experimental Biology*, **198**(7): 1509-1518.
- Hofmann, G. E. (1999). "Ecologically relevant variation in induction and function of heat shock proteins in marine organisms." *American Zoologist*, **39**(6): 889-900.
- Hofmann, G. E. (2005). "Patterns of Hsp gene expression in ectothermic marine organisms on small to large biogeographic scales." *Integrative and Comparative Biology*, **45**(2): 247-255.
- Laas, A. and Vosloo, A. (2010). "Exploring basic biochemical constituents in the body tissues of South African abalone *Haliotis midae* reared in shore-based mariculture systems." *African Journal of Marine Science*, **32**(1): 55-63.
- Lee, A.-C. and Lee, K.-T. (2011). "The enzyme activities of opine and lactate dehydrogenases in the gills, mantle, foot, and adductor of the hard clam *Meretrix lusoria*." *Journal of Marine Science and Technology*, **19**(4): 361-367.
- Lewis, S., Handy, R. D., Cordi, B., Billinghamurst, Z. and Depledge, M. H. (1999). "Stress proteins (HSP's): methods of detection and their use as an environmental biomarker." *Ecotoxicology*, **8**(5): 351-368.
- Livak, K. J. and Schmittgen, T. D. (2001). "Analysis of relative gene expression data using real-time quantitative PCR and the $2^{-\Delta\Delta CT}$ method." *Methods*, **25**(4): 402-408.
- Livingstone, D. R. (1991). "Origins and evolution of pathways of anaerobic metabolism in the animal kingdom." *American Zoologist*, **31**(3): 522-534.
- Lyon, R. G. (1995). "Aspects of the physiology of the South African abalone *Haliotis midae* L., and implications for intensive abalone culture". M.Sc. Thesis, Rhodes University.
- Mayzaud, P. and Conover, R. J. (1988). "O:N atomic ratio as a tool to describe zooplankton metabolism." *Marine Ecology Progress Series*, **45**(3): 289-302.
- McDonagh, B., Tyther, R. and Sheehan, D. (2005). "Carbonylation and glutathionylation of proteins in the blue mussel *Mytilus edulis* detected by proteomic analysis and Western blotting: Actin as a target for oxidative stress." *Aquatic Toxicology*, **73**(3): 315-326.
- Mukhopadhyay, I., Nazir, A., Saxena, D. K. and Chowdhuri, D. K. (2003). "Heat shock response: hsp70 in environmental monitoring." *Journal of Biochemical and Molecular Toxicology*, **17**(5): 249-254.
- Naylor, M. A., Kaiser, H. and Jones, C. L. W. (2011). "The effect of dietary protein level on total ammonia nitrogen and free ammonia nitrogen concentrations in a serial-use raceway used to farm South African abalone, *Haliotis midae* Linnaeus, 1758." *Journal of Shellfish Research*, **30**(2): 337-341.
- Nyström, T. (2005). "Role of oxidative carbonylation in protein quality control and senescence." *EMBO Journal*, **24**(7): 1311-1317.

- O'Omolo, S., Gäde, G., Cook, P. A. and Brown, A. C. (2003). "Can the end products of anaerobic metabolism, tauripine and D-lactate, be used as metabolic stress indicators during transport of live South African abalone *Haliotis midae*?" African Journal of Marine Science, **25**(1): 301-309.
- Osovitz, C. J. and Hofmann, G. E. (2005). "Thermal history-dependent expression of the hsp70 gene in purple sea urchins: Biogeographic patterns and the effect of temperature acclimation." Journal of Experimental Marine Biology and Ecology, **327**(2): 134-143.
- Perry, A. L., Low, P. J., Ellis, J. R. and Reynolds, J. D. (2005). "Climate change and distribution shifts in marine fishes." Science, **308**(5730): 1912-1915.
- Podrabsky, J. E. and Somero, G. N. (2004). "Changes in gene expression associated with acclimation to constant temperatures and fluctuating daily temperatures in an annual killifish *Austrofundulus limnaeus*." Journal of Experimental Biology, **207**(13): 2237-2254.
- Pörtner, H. O. (2002). "Climate variations and the physiological basis of temperature dependent biogeography: systemic to molecular hierarchy of thermal tolerance in animals." Comparative Biochemistry and Physiology - Part A: Molecular & Integrative Physiology, **132**(4): 739-761.
- Pörtner, H. O. (2008). "Ecosystem effects of ocean acidification in time of ocean warming: a physiologist's view." Marine Ecology Progress Series, **373**: 203-217.
- Pörtner, H. O. and Farrell, A. P. (2008). "Physiology and climate change." Science, **322**(5902): 690-692.
- Pörtner, H. O. and Knust, R. (2007). "Climate change affects marine fishes through the oxygen limitation of thermal tolerance." Science, **315**(5808): 95-97.
- Pörtner, H. O., Mark, F. C. and Bock, C. (2004). "Oxygen limited thermal tolerance in fish?: answers obtained by nuclear magnetic resonance techniques." Respiratory Physiology & Neurobiology, **141**(3): 243-260.
- Proudfoot, L.-A. (2007). "Population structure, growth and recruitment of two exploited infralittoral molluscs (*Haliotis midae* and *Turbo sarmaticus*) along the south east coast, South Africa". M.Sc. Thesis, Rhodes University.
- Randall, D. J. and Tsui, T. K. N. (2002). "Ammonia toxicity in fish." Marine Pollution Bulletin, **45**(1-12): 17-23.
- Reddy-Lopata, K., Auerswald, L. and Cook, P. (2006). "Ammonia toxicity and its effect on the growth of the South African abalone *Haliotis midae* Linnaeus." Aquaculture, **261**(2): 678-687.
- Rouault, M., Pohl, B. and Penven, P. (2010). "Coastal oceanic climate change and variability from 1982 to 2009 around South Africa." African Journal of Marine Science, **32**(2): 237-246.
- Sales, J. and Britz, P. J. (2001). "Research on abalone (*Haliotis midae* L.) cultivation in South Africa." Aquaculture Research, **32**(11): 863-874.

- Sanders, B. M. (1993). "Stress proteins in aquatic organisms: an environmental perspective." *Critical Reviews in Toxicology*, **23**(1): 49-75.
- Scandalios, J. (2005). "Oxidative stress: molecular perception and transduction of signals triggering antioxidant gene defenses." *Brazilian Journal of Medical and Biological Research*, **38**(7): 995-1014.
- Snyder, M. J., Girvetz, E. and Mulder, E. P. (2001). "Induction of marine mollusc stress proteins by chemical or physical stress." *Archives of Environmental Contamination and Toxicology*, **41**(1): 22-29.
- Solórzano, L. (1969). "Determination of ammonia in natural waters by the phenolhypochlorite method." *Limnology and Oceanography*, **14**(5): 799-801.
- Somero, G. (2005). "Linking biogeography to physiology: evolutionary and acclimatory adjustments of thermal limits." *Frontiers in Zoology*, **2**(1): 1-9.
- Somero, G. N. (1995). "Proteins and temperature." *Annual Review of Physiology*, **57**(1): 43-68.
- Sørensen, J. G., Kristensen, T. N. and Loeschcke, V. (2003). "The evolutionary and ecological role of heat shock proteins." *Ecology Letters*, **6**(11): 1025-1037.
- Tomanek, L. (2008). "The importance of physiological limits in determining biogeographical range shifts due to global climate change: the heat-shock response." *Physiological and Biochemical Zoology*, **81**(6): 709-717.
- Tomanek, L. (2010). "Variation in the heat shock response and its implication for predicting the effect of global climate change on species' biogeographical distribution ranges and metabolic costs." *Journal of Experimental Biology*, **213**(6): 971-979.
- Tomanek, L. and Somero, G. N. (2002). "Interspecific- and acclimation-induced variation in levels of heat-shock proteins 70 (hsp70) and 90 (hsp90) and heat-shock transcription factor-1 (HSF1) in congeneric marine snails (genus *Tegula*): implications for regulation of hsp gene expression." *Journal of Experimental Biology*, **205**(5): 677-685.
- Tomanek, L. and Zuzow, M. J. (2010). "The proteomic response of the mussel congeners *Mytilus galloprovincialis* and *M. trossulus* to acute heat stress: implications for thermal tolerance limits and metabolic costs of thermal stress." *Journal of Experimental Biology*, **213**(20): 3559-3574.
- Troell, M., Robertson-Andersson, D., Anderson, R. J., Bolton, J. J., Maneveldt, G., Halling, C. and Probyn, T. (2006). "Abalone farming in South Africa: an overview with perspectives on kelp resources, abalone feed, potential for on-farm seaweed production and socio-economic importance." *Aquaculture*, **257**(1-4): 266-281.
- Van Aardt, W. and Booyens, J. (2004). "Water hardness and the effects of Cd on oxygen consumption, plasma chlorides and bioaccumulation in *Tilapia sparrmanii*." *Water SA*, **30**(1): 57-64.
- Vosloo, D., Sara, J. and Vosloo, A. (2012). "Acute responses of brown mussel (*Perna perna*) exposed to sub-lethal copper levels: Integration of physiological and cellular responses." *Aquatic Toxicology*, **106-107**(0): 1-8.

- Vosloo, D., van Rensburg, L. and Vosloo, A. (2013). "Oxidative stress in abalone: The role of temperature, oxygen and l-proline supplementation." *Aquaculture*, **416–417**(0): 265-271.
- Vosloo, D. and Vosloo, A. (2010). "Response of cold-acclimated, farmed South African abalone (*Haliotis midae*) to short-term and long-term changes in temperature." *Journal of Thermal Biology*, **35**(7): 317-323.
- Vosloo, D., Vosloo, A., Morillion, E. J., Samuels, J. N. and Sommer, P. (2013). "Metabolic readjustment in juvenile South African abalone (*Haliotis midae*) acclimated to combinations of temperature and dissolved oxygen levels." *Journal of Thermal Biology*, **38**(7): 458-466.
- Wells, R. M. G. and Baldwin, J. (1995). "A comparison of metabolic stress during air exposure in two species of New Zealand abalone, *Haliotis iris* and *Haliotis australis*: implications for the handling and shipping of live animals." *Aquaculture*, **134**(3–4): 361-370.
- Wright, P. A. (1995). "Nitrogen excretion: three end products, many physiological roles." *Journal of Experimental Biology*, **198**(2): 273-281.

6. APPENDIX

A. Recipes

A.1. Phenol-Hypochlorite Method

A.1.1. Phenol Solution: 10 g phenol made up to a final volume of 100 mL in 95% (v/v) ethanol and stored at 4°C.

95% Ethanol

Reagent	500 mL Volume
100% Ethanol	475 mL
Distilled H ₂ O	25 mL

Distilled water was added to ethanol to yield a final volume of 500 mL.

A.1.2 Sodium Nitroprusside: 1 g of sodium nitroprusside made up to 200 mL with distilled water and stored at 4°C in an amber bottle.

A.1.3. Alkaline Solution: 100 g tri-sodium citrate and 5 g sodium hydroxide made up to 500 mL with distilled water and stored at 4°C in an amber bottle.

A.1.4. Oxidizing Solution: Commercial bleach and alkaline solution (1:4) made up on the day according to number of determinations required (stable for only 12 hours).

Approximation of amount of oxidizing solution to make up:

Number of determinations	Bleach (mL)	Alkaline solution (mL)
10 (using 5 mL samples)	1.0	4.0
12	1.25	5.0
15	1.5	6.0
20	2.0	8.0
25	2.5	10.0

A.1.5. Standard Master Solution: 0.05349 g NH₄Cl made up to 1 L in distilled water (final concentration of 1 mM NH₄Cl). A few drops of chloroform were added as a preservative.

Amounts of Standard Master Solution required per standard:

Concentration of Standard (μM)	Standard Master Solution (μL)	Distilled Water (mL)
1	5	5
5	25	5
10	50	5
20	100	5
40	200	5

A.2. Dot Blotting Procedure

A.2.1. 1x Blocking Buffer

Reagent	50 mL Volume
1X Wash Buffer *	50 mL
Skimmed milk powder	2.5 g

Dried skimmed milk was dissolved in wash buffer to reach a final volume of 50 mL.

*See Appendix A.2.7 for recipe.

A.2.2. 1x Tris-Buffered Saline-Tween20 (TBS-T) Wash Buffer

Reagent	1 L Volume
10X TBS Buffer Stock *	100 mL
Distilled water	900 mL
Tween20	1000 μL

Tween20 was added to an aliquot of 10X TBS Buffer which was then diluted in distilled water to a final volume of 1 L.

*TBS Buffer Stock recipe below

10x Tris-Buffered Saline (TBS) Buffer Stock

Reagent	1 L Volume
NaCl	80 g
Tris-HCl	31.52 g
Distilled water	1 L

Distilled water was added to NaCl and Tris-HCl to make a final volume of 1 L.

A.2.3. 1x Ponceau S Stain

Reagent	500 mL Volume
Ponceau S	0.5 g
Acetic acid	5 mL
Distilled water	495 mL

Acetic acid was added to Ponceau S and the solution made up to 500 mL using distilled water.

1% Acetic Acid Destain

Reagent	500 mL Volume
Acetic acid	5 mL
Distilled water	495 mL

Acetic acid was diluted in distilled water to yield a volume of 500 mL.

A.2.4. Troubleshooting procedure for optimizing Hsp70 detection

The activity and specificity of the Hsp70 primary antibody has previously been shown (Honors project, 2011; see Figure A.2.4.1. below).

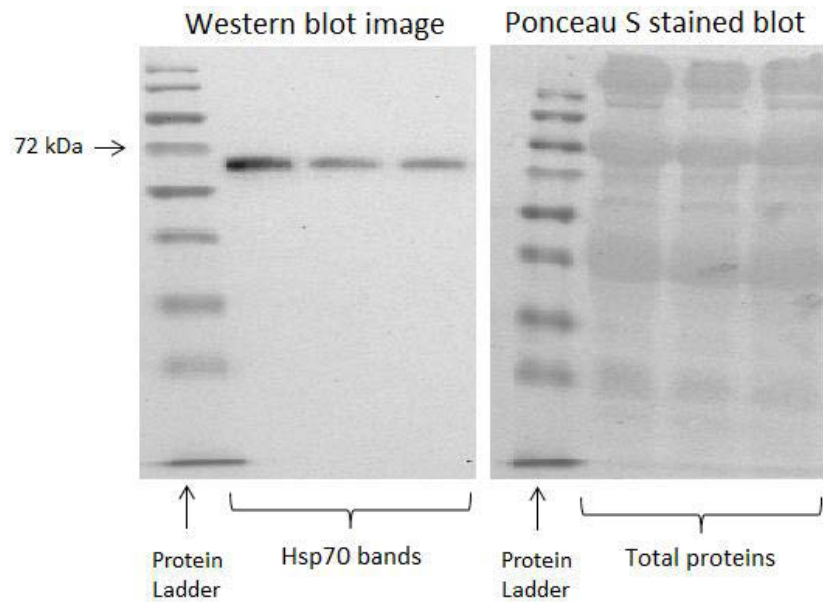


Figure A.2.4.1: Validation of the action and specificity of the Hsp70 primary antibody.

Western blots performed using West coast or East coast samples did not show positive binding of the Hsp70 proteins with the antibodies (see Figure A.2.4.2. below). The presence of the molecular weight marker confirms effective transfer while the Ponceau S stained image shows the presence of proteins.

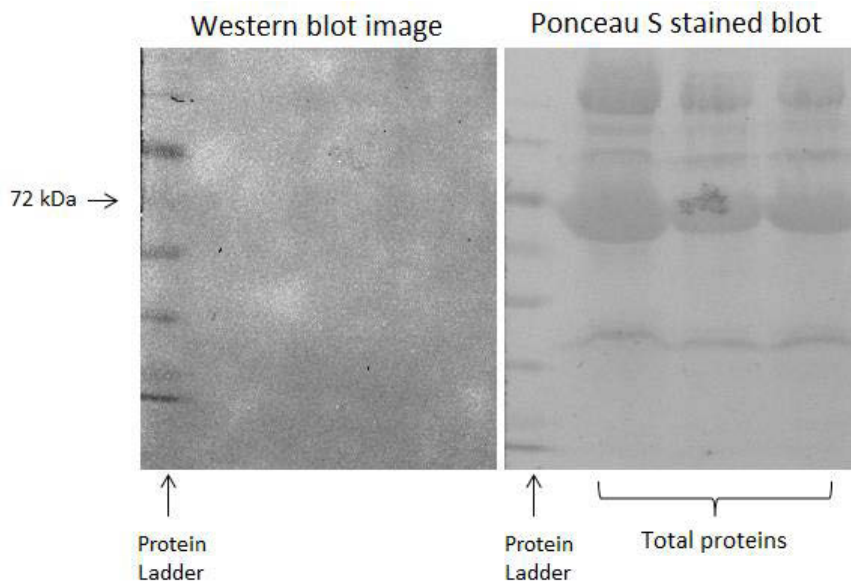


Figure A.2.4.2: Validation of effective transfer and presence of protein on Western blots

To rule out the possibility of protein sample loss during the transfer process, dot blots were used to confirm to binding of Hsp70 proteins to antibodies, by eliminating the transfer

process altogether. Dots blots produced however, did not produce protein dots with high enough signal to be detected due to excessive background noise (refer to Figure 3.3.1. of Results section). The blocking time was then increased from 45 minutes to 60 minutes; this modification however, did not yield positive results (Figure A.2.4.3.)

(*Note subsequent dot blots represent fewer protein dots in an attempt to conserve protein samples and reduce inter-sample variation.)

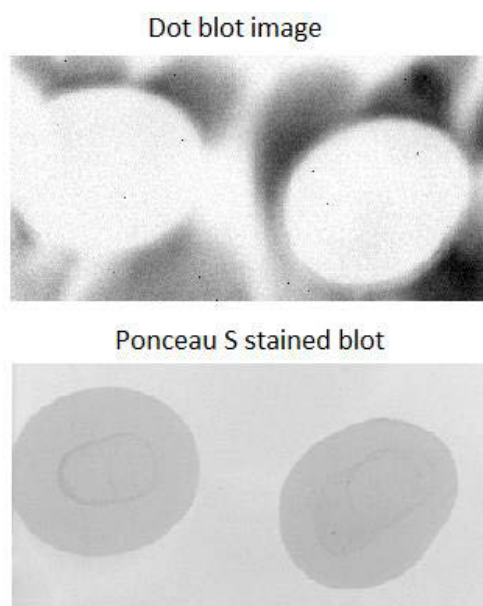


Figure A.2.4.3: Dot blot of a selected protein samples with accompanying Ponceau S stained blot. Dot blot image conveys high levels of background signal.

Primary antibody was diluted in an attempt to reduce the signal-to-noise ratio. This was done by serially diluting the 1:500 antibody stock solution to yield a 1:1000 (a), 1:2500 (b), 1:5000 (c), 1:7500 (d) and 1:10000 (e) dilution. This dilution series was repeated by diluting the secondary antibody with neither dilution producing favorable results.

Following the lack of success with either of the antibody dilutions, the length of washes was increased in order to reduce background and obtain a stronger signal. Washes were as follows: i) 3 x 10 minute washes (TBS-T) following primary antibody incubation and ii) 1 x 15 minute and 2 x 10 minute washes (TBS-T) ending in 1 x 10 minute wash (TBS) after incubation in secondary antibody. Increased washes reduced protein-antibody binding such that chemiluminescence was not detected by the imaging system (Figure A.2.9.4.),

suggesting that amounts of protein bound to membranes was so low that normal background signal appeared as being high.

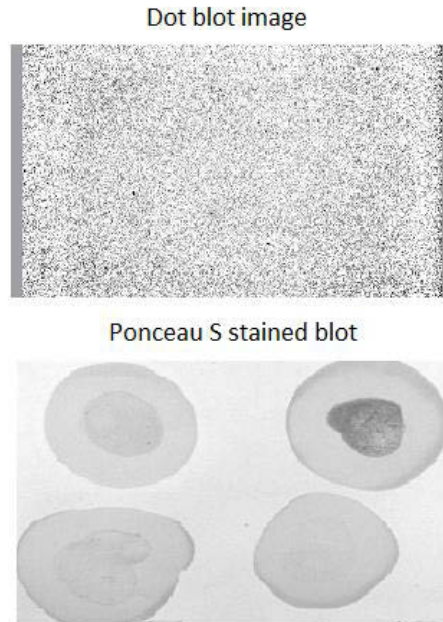


Figure A.2.4.4: Dot blot from which no signal was detected as a result of extended washing. Presence of protein confirmed by Ponceau S stained blot.

A.3. RNA Extraction and Integrity Assessment

A.3.1. 1x Phosphate-Buffered Saline (PBS)

Reagent	500 mL Volume
Sodium Dihydrate Phosphate	2.184 g
Disodium Hydrate Phosphate	6.407 g
NaCl	4.375 g
Distilled water	500 mL

Sodium dihydrate phosphate and disodium hydrate phosphate were dissolved in 250 mL of distilled water. The pH of the solution was adjusted to 7.2 and the solution then made up to a final volume of 500 mL. Once prepared the solution was autoclaved and allowed to cool before use.

A.3.2. 75% Ethanol

Reagent	50 mL Volume
100% Ethanol	37.5 mL
Distilled H ₂ O	12.5 mL

Distilled water was added to ethanol to reach a final volume of 50 mL.

A.3.3. DEPC-treated Water

Reagent	1 L Volume
DEPC	100 µL
Distilled H ₂ O	1 L

DEPC was added to distilled water and the solution incubated at 37°C for 2 hr. The solution was then autoclaved and allowed to cool before use.

A.3.4. DEPC-treated 1.2% Agarose Gel

Reagent	110 mL Volume
Agarose	0.36 g
DEPC-treated 1x TBE Buffer *	30 mL
Ethyidium bromide (10 mg/mL)	4.5 µL

Under a fume hood, DEPC-treated 1x TBE buffer was added to agarose to reach a final volume 30 mL. The solution was heated to dissolve the agarose and once slightly cooled the ethyidium bromide was added.

*See Appendix A.3.5. for recipe.

A.3.5. DEPC-treated 10x Tris-Borate-EDTA (TBE) Buffer Stock

Reagent	1 L Volume
Tris-Base	107.78g
Boric acid	55.02 g
EDTA	3.722 g
DEPC-treated water	1 L

Tris-Base, Boric acid and EDTA was dissolved in DEPC-treated water to reach a volume of 1 L.

DEPC-treated 1x Tris-Borate-EDTA (TBE) Buffer

Reagent	500 mL Volume
10x TBE Buffer	50 mL
DEPC-treated water	450 mL

The TBE Buffer stock was diluted (1:10) using DEPC-treated water to yield a final volume of 500 mL.

A.4. PCR Product Electrophoresis

A.4.1. 1.2% Agarose Gel

Reagent	30 mL Volume
Agarose	0.36 g
1x TBE Buffer *	30 mL
Ethydium bromide (10 mg/mL)	4.5 µL

Agarose was dissolved in 1x TBE buffer, made up to a final volume of 30 mL, by heating. Once dissolved the gel solution was allowed to cool before the ethyidium bromide was added.

*See Appendix A.4.2. for recipe.

A.4.2. 10x Tris-Borate-EDTA (TBE) Buffer Stock

Reagent	1 L Volume
Tris-Base	107.78g
Boric acid	55.02 g
EDTA	3.722 g
Distilled water	1 L

The dry reagents were dissolved in distilled water and the buffer made up to a final volume of 1 L.

1x Tris-Borate-EDTA (TBE) Buffer

Reagent	500 mL Volume
10x TBE Buffer	50 mL
Distilled water	450 mL

The TBE buffer stock was diluted (1:10) using distilled water to yield a volume of 500 mL.

B. MIQE Guidelines

Below is a list of information representing the minimum that is required for evaluating qPCR experiments as outlined by the Minimum Information for Publication of Quantitative Real-Time PCR Experiments (MIQE) guidelines (Bustin *et al.*, 2009). These guidelines were designed to assess the validity of the results generated by qPCR experiments and to ensure that consistency is maintained across laboratories.

B.1. Experimental Design

Hsp70 primers were used to assess the effect of thermal stress on the expression of the *hsp70* gene. The internal reference gene used, *coxIII*, was selected as its expression is not affected by changes in temperature (Vosloo *et al.*, 2013). To evaluate the changes in *hsp70* gene expression abalone were exposed to two thermal treatments. The first consisted of fluctuations that were 2°C greater than and less than control temperatures (16°C±2), while the second treatments consisted of fluctuations 4°C above and below that of the control temperatures (16°C±4). All groups were thus exposed to a mean temperature of 16°C, while that of the control group was kept constant.

B.2. RNA Extraction and cDNA Synthesis

Foot muscle was used as the preferred tissue for the extraction of RNA using the TRI reagent protocol (refer to section 2.9.1. of Materials and Methods). RNA integrity was confirmed by agarose gel electrophoresis (see section 3.4.1. of Results section) and the concentration determined by UV-spectrophotometer (NanoDrop ND-1000). Once the concentration had been determined 2 µg of RNA were used for the construction of cDNA (section 2.9.2 of Materials and Methods). SuperScript™ III RT was excluded from selected reactions to produce no reverse transcriptase (noRT) controls for subsequent PCR and qPCR reactions. Reactions where cDNA was substituted with 1 µL of Nuclease-free water acted as the no template (NTC) controls.

B.3. qPCR Protocol

Target genes were amplified using SYBR[®] Green Jumpstart[™] Taq ReadyMix[™] (Sigma), where each reaction contained 12.5 μ L of SYBR[®] Green JumpStart[™] Taq ReadyMix[™] (Sigma), 10.5 μ L of Nuclease-free water (Promega), 1 μ L of cDNA and 0.5 μ L each of forward and reverse primer. The primers used for each reaction were those for *hsp70* (target gene) and *coxIII* (reference gene). The protocol used (Figure B.3.1) was as outlined by Vosloo *et al.* (2013) (refer to section 2.10. of Materials and Methods for details of cycling conditions) and yielded two discrete amplification curves of the target and reference genes (Figure B.3.2.).

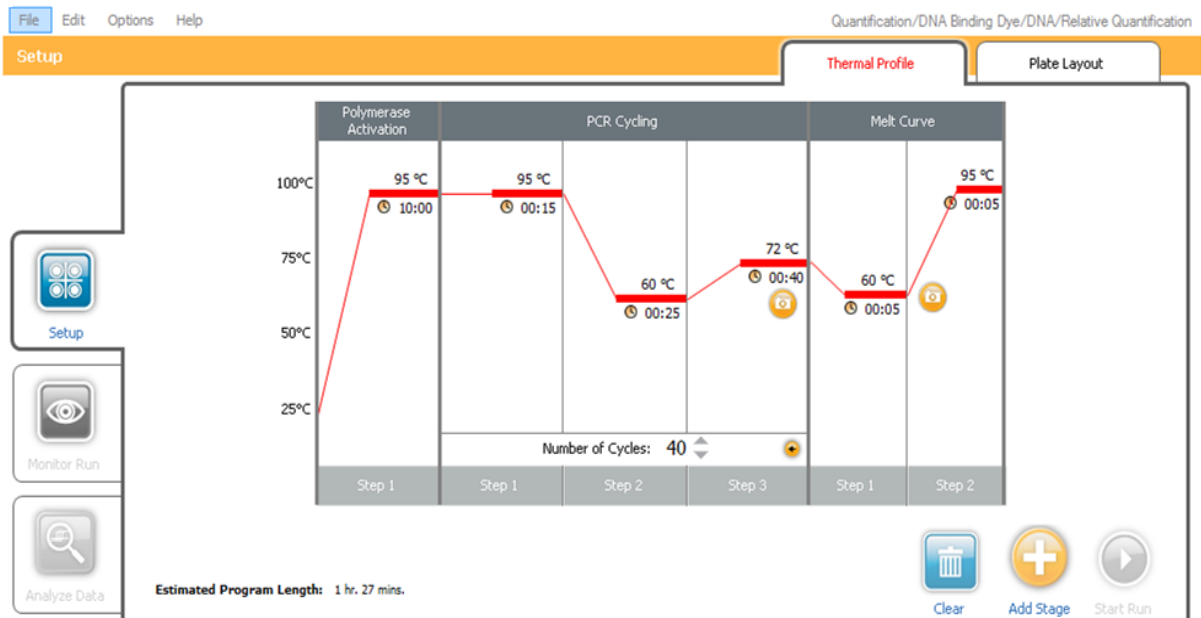


Figure B.3.1: Protocol used to perform all qPCR reactions outlined by Vosloo *et al.* (2013) and created using the Eco™ Software (v3.0.16.0).

Amplification Plot

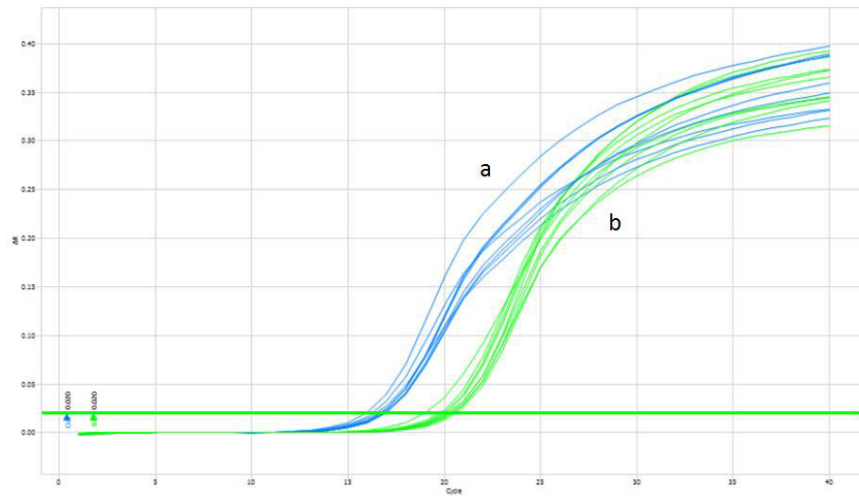


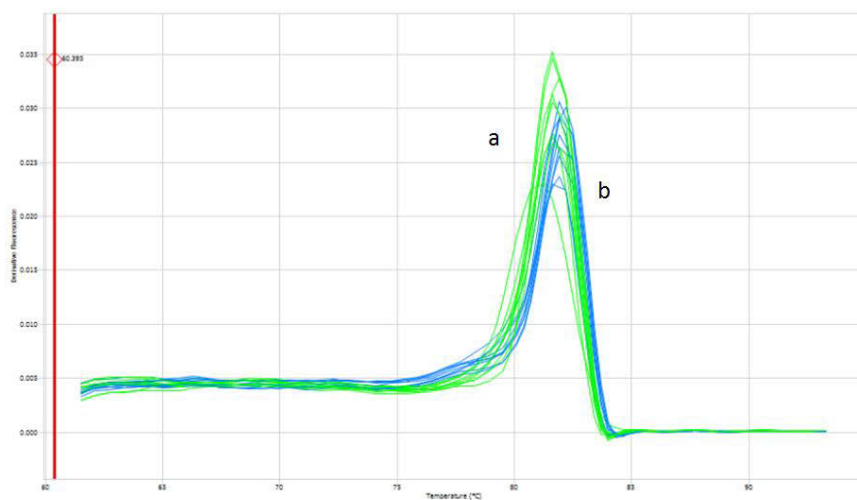
Figure B.3.2: Fluorescence curves representing (a) *coxIII* and (b) *hsp70* amplification.

B.4. qPCR Validation

B.4.1. Melt Analysis Validation

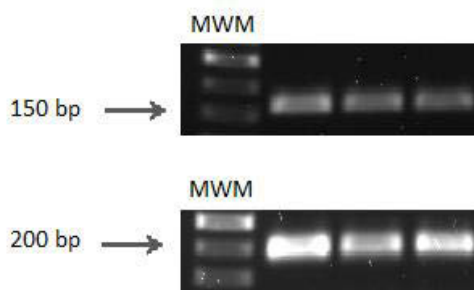
Verification of the production of a single product from each primer set was verified by melt curve analysis and agarose gel electrophoresis. Each set of primers used produced a single melt curve (Figure B.4.1. i) which corresponded to single melting temperature (Figure B.4.1. ii) and yielded a single band when qPCR products were electrophoresed on agarose gels (Figure B.4.1. ii).

Melt Curve



i)

Well	Assay Name	Assay Role	Tm1	Tm2	Tm3
D1	Cox	Unknown	81.9	N/A	N/A
D2	Cox	Unknown	81.9	N/A	N/A
D3	Cox	Unknown	81.9	N/A	N/A
D4	Hsp	Unknown	81.6	N/A	N/A
D5	Hsp	Unknown	81.6	N/A	N/A
D6	Hsp	Unknown	81.6	N/A	N/A



ii)

Figure B.4.1: i) Curves representing melt for (a) *hsp70* and (b) *coxIII*. ii) Accompanying melt temperature data (control data shown only) and validation by agarose gel electrophoresis showing *coxIII* (150 bp) and *hsp70* (200 bp) bands.

B.4.2. Assessment of qPCR Reaction Efficiency

The reaction efficiencies of the target genes were assessed by a serial dilution (10x) of the cDNA templates followed by amplification using the above stated qPCR protocol (Figure B.3.1.). The mean C_T value for each target gene was then plotted against the cDNA dilutions (Figure B.4.2.). The gradient of the linear slope produced should be close to zero and $R^2 > 0.98$ should be obtained when using the $2^{-\Delta\Delta C_T}$ method (Livak and Schmittgen, 2001).

The reaction efficiency of the gene of interest (*hsp70*) should be equal to that of the reference gene (*coxIII*) and both should occur between 90% and 110% (Livak and Schmittgen, 2001). These values were generated using an online calculator found at: <http://www.genomics.agilent.com/biocalculators/calcSlopeEfficiency.jsp>, by inputting the gradient of the slope.

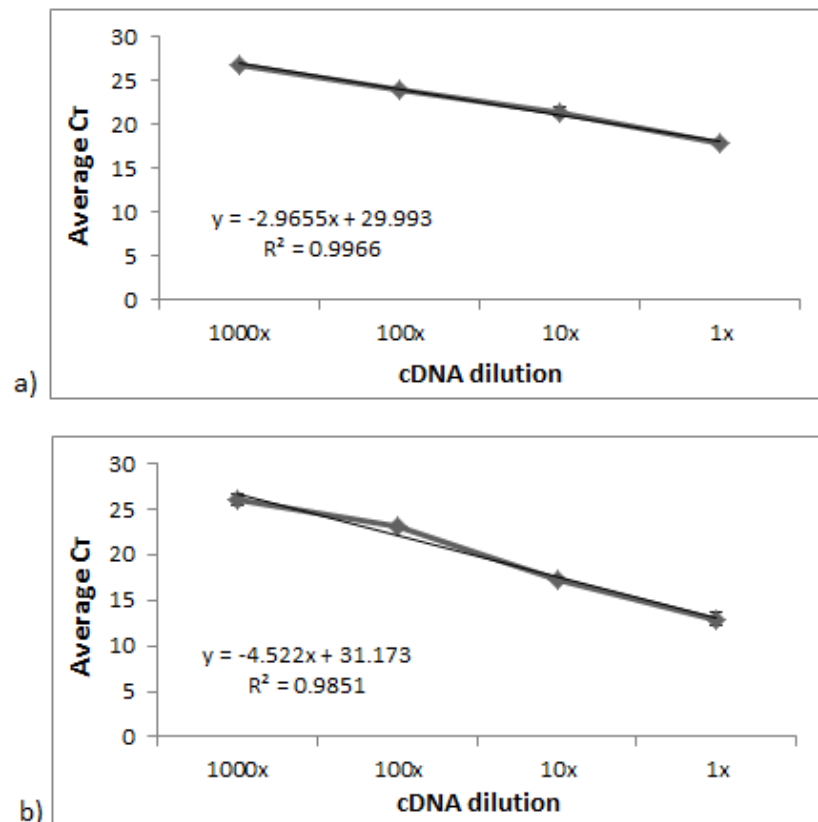


Figure B.4.2: Assessment of efficiency curves for *coxIII* (a) where $R^2 = 0.9966$ with a corresponding reaction efficiency of 117.4%, and for *hsp70* (b) where $R^2 = 0.9851$ and had a corresponding reaction efficiency of 66.4%.

Although the *hsp70* primers did not yield a reaction efficiency within the desired range (between 90% and 110%) they were still capable of amplifying the region of interest as shown by the formation of qPCR product within the correct range (refer to Figure B.4.1. ii.). For publication purposes however, primers with a greater reaction efficiency would need to be designed as stipulated by the MIQE guidelines (Bustin *et al.*, 2009).

B.5. Data Analysis

Data was analyzed using the Eco™ Software (v3.0.16.0) and all readings were taken at a baseline fluorescence of 0.2 RFU. Data points were excluded if the C_T values were: greater than 38, or the standard deviation of the triplicate group was greater than 0.5.

B.5.1. The $2^{-\Delta\Delta C_T}$ Method

The $2^{-\Delta\Delta C_T}$ method enables the calculation of the fold change of the gene of interest relative to the reference gene (Livak and Schmittgen, 2001). Reactions were done in triplicate, and the mean C_T and standard deviation determined for each reaction. The mean C_T of the reference gene was then subtracted from that of the gene of interest to yield the ΔC_T . The ΔC_T for the control was then subtracted from those of the treatment groups thus producing $\Delta\Delta C_T$. The negative of this value was then expressed to the base 2 such that the $2^{-\Delta\Delta C_T}$ of the control group always yields 1 and the treatment groups expressed as fold changes relative to this. Statistical analyses of these fold changes were then performed by One-Way ANOVA using SPSS® Statistics Version 21 (IBM®).